RESEARCH ARTICLE

Biochemical and Immunological Characterization of Truncated Fragments of the Receptor-Binding Domains of *C. difficile* Toxin A

Jui-Hsin Huang[1,2], Zhe-Qing Shen[1], Shu-Pei Lien[1], Kuang-Nan Hsiao[1], Chih-Hsiang Leng[1], Chi-Chang Chen[1], Leung-Kei Siu[1], Pele Choi-Sing Chong[1,2,3]*

1 Vaccine R&D Center, National Institute of Infectious Diseases and Vaccinology, National Health Research Institutes, Zhunan Town, Miaoli County, Taiwan, 2 Graduate Institute of Life Science, National Defense Medical Center, Taipei, Taiwan, 3 Graduate Institute of Immunology, China Medical University, Taichung, Taiwan

* pelechong@nhri.org.tw

Abstract

Clostridium difficile is an emerging pathogen responsible for opportunistic infections in hospitals worldwide and is the main cause of antibiotic-associated pseudo-membranous colitis and diarrhea in humans. Clostridial toxins A and B (TcdA and TcdB) specifically bind to unknown glycoprotein(s) on the surface of epithelial cells in the host intestine, disrupting the intestinal barrier and ultimately leading to acute inflammation and diarrhea. The C-terminal receptor-binding domain (RBD) of TcdA, which is responsible for the initial binding of the toxin to host glycoproteins, has been predicted to contain 7 potential oligosaccharide-binding sites. To study the specific roles and functions of these 7 putative lectin-like binding regions, a consensus sequence of TcdA RBD derived from different *C. difficile* strains deposited in the NCBI protein database and three truncated fragments corresponding to the N-terminal (residues 1–411), middle (residues 296–701), and C-terminal portions (residues 524–911) of the RBD (F1, F2 and F3, respectively) were designed and expressed in *Escherichia coli*. In this study, the recombinant RBD (rRBD) and its truncated fragments were purified, characterized biologically and found to have the following similar properties: (a) are capable of binding to the cell surface of both Vero and Caco-2 cells; (b) possess Toll-like receptor agonist-like adjuvant activities that can activate dendritic cell maturation and increase the secretion of pro-inflammatory cytokines; and (c) function as potent adjuvants in the intramuscular immunization route to enhance immune responses against weak immunogens. Although F1, F2 and F3 have similar repetitive amino acid sequences and putative oligosaccharide-binding domains, they do not possess the same biological and immunological properties: (i) TcdA rRBD and its fragments bind to the cell surface, but only TcdA rRBD and F3 internalize into Vero cells within 15 min; (ii) the fragments exhibit various levels of hemagglutinin (HA) activity, with the exception of the F1 fragment, which demonstrates no HA activity; and (iii) in the presence of alum, all fragments elicit various levels of anti-toxin A-neutralizing antibody responses, but those neutralizing antibodies elicited by

F2 did not protect mice against a TcdA challenge. Because TcdA rRBD, F1 and F3 formulated with alum can elicit immune protective responses against the cytotoxicity of TcdA, they represent potential components of future candidate vaccines against *C. difficile*-associated diseases.

Introduction

Opportunistic nosocomial infection in hospitalized patients is often related to *Clostridium difficile* infection (CDI) that develops via disruption of the balance of the intestinal micro-flora by antibiotic therapies used during hospitalization. Thus, CDI often results in *Clostridium difficile*-associated diseases (CDAD), such as diarrhea, pseudomembranous colitis, and toxic mega-colon [1,2]. In the past two decades, CDI has become a serious emerging infectious disease worldwide due to a significant increase in multi-drug resistance [3]. Moreover, the discovery of a hyper-virulent and antibiotic-resistant epidemic strain, NAP1/027, in developed countries poses a major challenge for CDAD prevention [4,5]. More importantly, *C. difficile* relapse is approximately 15–35% within a few weeks despite standard CDI therapy employing either vancomycin or metronidazole [6]. The pathogenicity of CDI is largely correlated to the clostridial toxins, toxin A and toxin B (TcdA and TcdB), that are secreted in the gastrointestinal environment of infected hosts and disrupt epithelial cell barriers in the small intestine [7]. Both toxins consist of a holotoxin with multi-functional domains that mediate *C. difficile* pathogenesis. The mechanism underlying TcdA and TcdB toxicity involves three steps: (a) binding to an unidentified receptor protein(s) on the surface of the intestinal epithelium and internalization through its C-terminal receptor-binding domain, (b) auto-cleavage and translocation of the N-terminal glucosyltransferase domain into the cytosol from the endosomal membrane; and (c) use of the N-terminal enzymatic region to inactivate the Rho GTPase family via glycosylation [8–10].

The published literature has indicated that TcdA-specific antibodies in patient sera positively correlated with the prevention of CDAD recurrence [11–15]. Therefore, passive immunization with anti-toxin antibodies has been shown to confer protection against CDI in murine models, and TcdA-specific monoclonal antibodies are currently being tested in clinical trials [11,16–19]. In addition, different *C. difficile* vaccine strategies are being evaluated; the most advanced strategy is vaccination with formalin-inactivated toxins [11, 20–21]. Immunization using the receptor-binding domain (RBD) of *C. difficile* toxins as the antigen in formulation with different adjuvants has been shown to elicit toxin-neutralizing antibody responses and protect mice against toxin or bacteria challenges [22–29]. The RBD is predicted to have a molecular size of approximately 100 kDa and is composed of 32–38 homologous repetitive peptides, depending on the sequence analysis [30–31]. Based on the crystal structure, the RBD was predicted to consist of 32 short repeat and 7 long repeat carbohydrate-binding sites [31]. The specific roles and functions of the 7 putative carbohydrate-binding regions are unclear, but they correlate to the binding of the oligosaccharide Galα1-3Galβ1-4GlcNAc [32–35]. Greco et al. [32] was the first to localize carbohydrate binding to the junction of 2 short repeats and a long repeat. The TcdB RBD has approximately 530 amino acids and 4 putative oligosaccharide-binding sites [33]. Interestingly, among *C. difficile* strains deposited in the NCBI database, the amino acid sequences of the putative oligosaccharide-binding sites between TcdA and TcdB were found to share approximately 50 to 70% similarity [36]. To this end, we rationally designed two novel immunogens based on these putative oligosaccharide-binding sites of

TcdA RBD and TcdB RBD to induce broadly neutralizing antibodies against both toxins. The biochemical and immunological functions of the TcdB RBD have been characterized and published [36]. In this study, a recombinant TcdA RBD (rRBD) containing a consensus sequence of TcdA RBD identified from different *C. difficile* strains deposited in the NCBI protein database and three fragments corresponding to the N-terminal, middle, and C-terminal parts of RBD (F1, F2 and F3, respectively) were designed and expressed in *Escherichia coli*. The purified TcdA rRBD and its fragments were characterized biologically to establish a platform to study the specific roles and functions of the 7 putative receptor-binding regions. Mouse immunogenicity studies were performed to investigate the potential of the rRBD and/or its fragments as components of candidate vaccines against CDAD.

Materials and Methods

Ethics Statement

All experiments were conducted in accordance with the guidelines of the Laboratory Animal Center of the National Health Research Institutes (NHRI). Animal use protocols were reviewed and approved by the Institutional Animal Care and Use Committee of the National Health Research Institutes (approved protocol no. NHRI-IACUC-100053-A).

Design and construction of the consensus sequence of rRBD and its truncated fragments

RBD sequences from different *Clostridium difficile* strains deposited in the NCBI database were aligned for sequence analysis using the alignment tools from Vector NTI Advance 11.5 (Life Technologies, Carlsbad, CA). This consensus sequence was analyzed with online software (http://www.ebi.ac.uk/Tools/pfa/radar/) to detect repetitive protein sequences and predicted potential ligand-binding sites. The nucleotide sequence of TcdA rRBD was optimized for *E. coli* codon usage, chemically synthesized (GeneArt; Life Technologies) for cloning and expressed in *E. coli*. TcdA rRBD was inserted into a pET-22b vector (Novagen, Darmstadt, Germany) containing a poly-histidine tag at the 3'-end between NdeI and XhoI restriction sites. The resulting pET-22b_TcdA RBD construct was transformed into *E. coli* JM109 (DE3) (Promega, Madison, WI) for TcdA rRBD expression. TcdA rRBD was divided into three fragments, F1, F2 and F3, which correspond to the N-terminal residues 1 to 411, the middle region residues 296 to 701, and the C-terminal residues 524 to 911 of TcdA RBD (Fig 1A), respectively. The nucleotide sequences of the TcdA rRBD fragments containing a poly-histidine tag at the 3'-end were cloned into the pET-22b vector and transformed into *E. coli* JM109 (DE3) strain for protein expression.

Purification of rRBD and its truncated fragments

TcdA rRBD and its truncated fragments were individually expressed in *E. coli* JM109 (DE3) (Promega) grown in Luria-Bertani medium (LB medium) at 20°C for 16 h following induction with 1 mM isopropyl-β-D-thiogalacto-pyranoside (IPTG). The purification process for TcdA rRBD and its fragments is briefly described below. Cells from 2 liters of culture medium were harvested by centrifugation and stored at -20°C before re-suspension in lysis buffer (50 mM sodium phosphate buffer, pH 7.2, containing 250 mM NaCl and 5 mM imidazole). The cells were physically disrupted using a French Press (Constant System, Daventry, UK) at 27 kpsi, and the supernatant was collected by filtration through a 0.22-μm filter. The crude extract was directly applied onto a nickel affinity chromatography column (GE Healthcare, Uppsala, Sweden) for purification of TcdA rRBD at 4°C. After sequential washes with a low concentration of
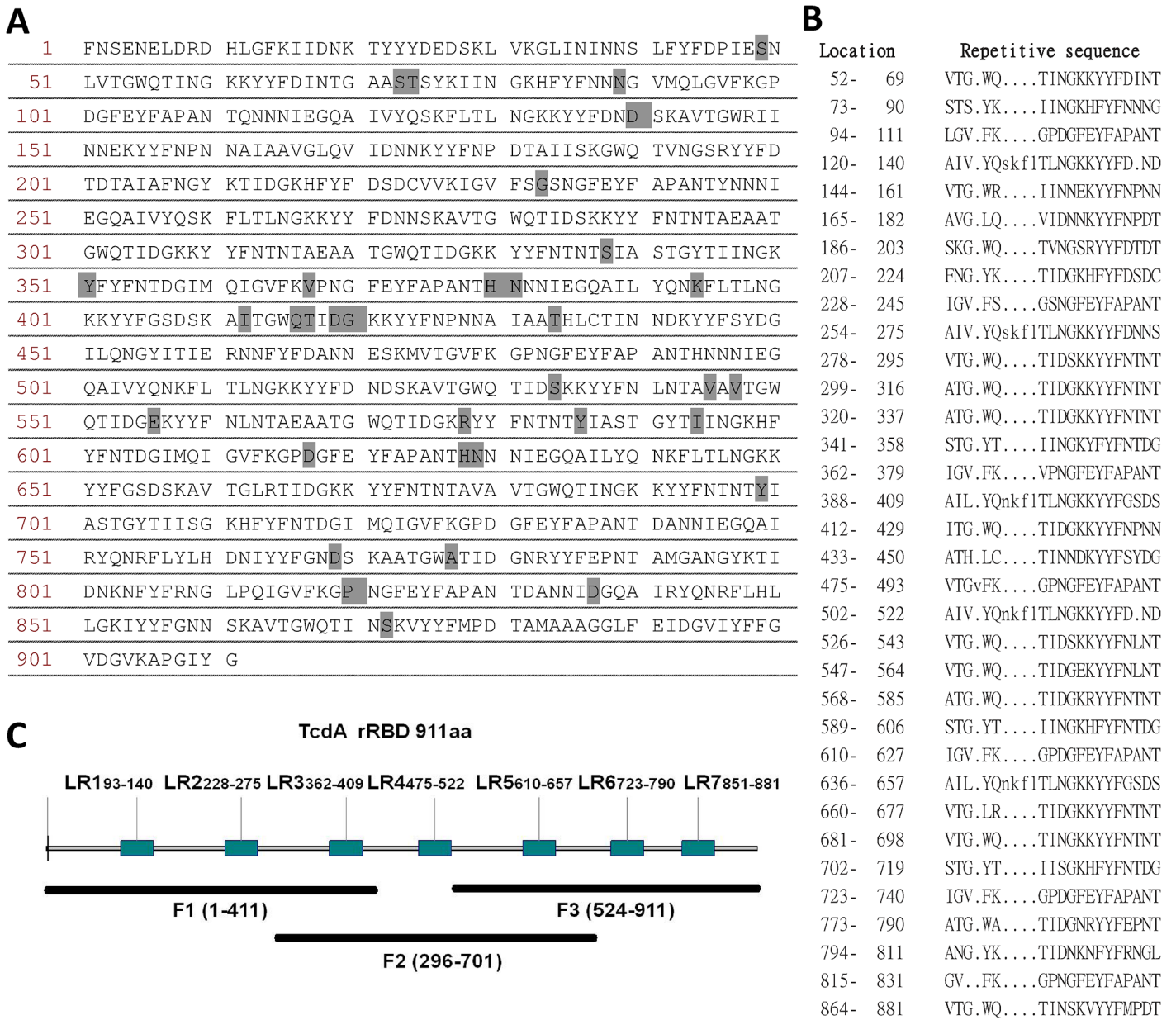
A

```
  1  FNSENELDRD HLGFKIIDNK TYYYDEDSKL VKGLININNS LFYFDPIESN
 51  LVTGWQTING KKYYFDINTG AASTSYKIIN GKHFYFNNNG VMQLGVFKGP
101  DGFEYFAPAN TQNNNIEGQA IVYQSKFLTL NGKKYYFDND SKAVTGWRII
151  NNEKYYFNPN NAIAAVGLQV IDNNKYYFNP DTAIISKGWQ TVNGSRYYFD
201  TDTAIAFNGY KTIDGKHFYF DSDCVVKIGV FSGSNGFEYF APANTYNNNI
251  EGQAIVYQSK FLTLNGKKYY FDNNSKAVTG WQTIDSKKYY FNTNTAEAAT
301  GWQTIDGKKY YFNTNTAEAA TGWQTIDGKK YYFNTNTSIA STGYTIINGK
351  YFYFNTDGIM QIGVFKVPNG FEYFAPANTH NNNIEGQAIL YQNKFLTLNG
401  KKYYFGSDSK AITGWQTIDG KKYYFNPNNA IAATHLCTIN NDKYYFSYDG
451  ILQNGYITIE RNNFYFDANN ESKMVTGVFK GPNGFEYFAP ANTHNNNIEG
501  QAIVYQNKFL TLNGKKYYFD NDSKAVTGWQ TIDSKKYYFN LNTAVAVTGW
551  QTIDGEKYYF NLNTAEAATG WQTIDGKRYY FNTNTYIAST GYTIINGKHF
601  YFNTDGIMQI GVFKGPDGFE YFAPANTHNN NIEGQAILYQ NKFLTLNGKK
651  YYFGSDSKAV TGLRTIDGKK YYFNTNTAVA VTGWQTINGK KYYFNTNTYI
701  ASTGYTIISG KHFYFNTDGI MQIGVFKGPD GFEYFAPANT DANNIEGQAI
751  RYQNRFLYLH DNIYYFGNDS KAATGWATID GNRYYFEPNT AMGANGYKTI
801  DNKNFYFRNG LPQIGVFKGP NGFEYFAPAN TDANNIDGQA IRYQNRFLHL
851  LGKIYYFGNN SKAVTGWQTI NSKVYYFMPD TAMAAAGGLF EIDGVIYFFG
901  VDGVKAPGIY G
```

B

Location		Repetitive sequence
52-	69	VTG.WQ....TINGKKYYFDINT
73-	90	STS.YK....IINGKHFYFNNNG
94-	111	LGV.FK....GPDGFEYFAPANT
120-	140	AIV.YQskflTLNGKKYYFD.ND
144-	161	VTG.WR....IINNEKYYFNPNN
165-	182	AVG.LQ....VIDNNKYYFNPDT
186-	203	SKG.WQ....TVNGSRYYFDTDT
207-	224	FNG.YK....TIDGKHFYFDSDC
228-	245	IGV.FS....GSNGFEYFAPANT
254-	275	AIV.YQskflTLNGKKYYFDNNS
278-	295	VTG.WQ....TIDSKKYYFNTNT
299-	316	ATG.WQ....TIDGKKYYFNTNT
320-	337	ATG.WQ....TIDGKKYYFNTNT
341-	358	STG.YT....IINGKYFYFNTDG
362-	379	IGV.FK....VPNGFEYFAPANT
388-	409	AIL.YQnkflTLNGKKYYFGSDS
412-	429	ITG.WQ....TIDGKKYYFNPNN
433-	450	ATH.LC....TINNDKYYFSYDG
475-	493	VTGvFK....GPNGFEYFAPANT
502-	522	AIV.YQnkflTLNGKKYYFD.ND
526-	543	VTG.WQ....TIDSKKYYFNLNT
547-	564	VTG.WQ....TIDGEKYYFNLNT
568-	585	ATG.WQ....TIDGKRYYFNTNT
589-	606	STG.YT....IINGKHFYFNTDG
610-	627	IGV.FK....GPDGFEYFAPANT
636-	657	AIL.YQnkflTLNGKKYYFGSDS
660-	677	VTG.LR....TIDGKKYYFNTNT
681-	698	VTG.WQ....TINGKKYYFNTNT
702-	719	STG.YT....IISGKHFYFNTDG
723-	740	IGV.FK....GPDGFEYFAPANT
773-	790	ATG.WA....TIDGNRYYFEPNT
794-	811	ANG.YK....TIDNKNFYFRNGL
815-	831	GV..FK....GPNGFEYFAPANT
864-	881	VTG.WQ....TINSKVYYFMPDT

C

TcdA rRBD 911aa

LR1 93-140 LR2 228-275 LR3 362-409 LR4 475-522 LR5 610-657 LR6 723-790 LR7 851-881

F1 (1-411)   F3 (524-911)

F2 (296-701)

Fig 1. The consensus sequence of the C-terminal repeats and putative receptor-binding domain from *C. difficile* toxin A (TcdA rRBD). (A) The amino acid sequence (911 residues) of TcdA rRBD was identified using online software (http://www.ebi.ac.uk/Tools/pfa/radar/). Sequence alignment with a reference TcdA (strain VPI10463) was performed, and the sequence differences are highlighted. (B) The localization and sequence of each short repeat are represented in the left and right columns. (C) The RBD fragments are F1 (residues 1–411), F2 (residues 296–701) and F3 (residues 524–911); the 7 lectin-like receptor-binding (LR) sites are putatively located at residues 93–140 (LR1), 228–275 (LR2), 362–409 (LR3), 475–522 (LR4), 610–657 (LR5), 723–790 (LR6) and 815–881 (LR7).

imidazole buffer, TcdA rRBD was eluted using a lysis buffer containing 500 mM imidazole. The eluent was then dialyzed in a 30-kDa cut-off dialysis bag against phosphate buffered saline (PBS), pH 7.2, containing 10% glycerol. To remove bacterial endotoxin, the TcdA rRBD solution was passed through an E membrane (Pall Corporation, Ann Arbor, MI). All purification steps were analyzed by 8% SDS-PAGE. The residual endotoxin was determined using the Limulus amoebocyte lysate (LAL) assay (Associates of Cape Cod, Inc., Cape Cod, MA).

Cell binding assay

Vero cells were seeded and cultured in 24-well plates using serum-free medium (VP-SFM) (Gibco, Carlsbad, CA) containing 4 mM glutamine at 37°C with 5% CO_2, and the cells were grown to confluence. Varying amounts of TcdA rRBD were added to the wells, and PBS was used as the negative control. After a 30-min incubation, the wells were washed twice with cold PBS. Radioimmunoprecipitation assay buffer (RIPA buffer) (Millipore, Billerica, MA), a strong cell lysis buffer, was added to the cells. The total cell lysate was analyzed by SDS-PAGE and then transferred onto polyvinylidene difluoride (PVDF) membranes (Pall Corporation) pre-soaked in methanol. PVDF membranes were blocked with 5% (w/v) nonfat dry milk in PBS and sequentially exposed to 0.5 μg/mL TcdA-specific monoclonal antibodies (Clone PCG-4; GeneTex, Taiwan) and 50 ng/mL horseradish peroxidase (HRP) conjugated to a secondary antibody (GeneTex) to detect the amount of TcdA rRBD bound to Vero cells. Antibodies were diluted in PBS containing 1% nonfat dry milk (w/v). PVDF membranes were washed twice at every step with PBST (1× PBS containing 0.05% Tween 20) at room temperature. Finally, signals were detected using enhanced chemiluminescence (ECL) according to the manufacturer's instructions (KPL, Gaithersburg, MD).

Immunofluorescence staining

Vero cells seeded in T-75 flasks with VP-SFM containing 4 mM glutamine at 37°C and 5% CO_2 were allowed to grow to 80% confluence. Cells were isolated and suspended with VP-SFM culture medium at 2×10^5 cells/mL inside a flow tube. Various amounts of either TcdA rRBD or its fragments were mixed with the cells and incubated at 37°C for 5, 15, and 30 min, and cell binding was stopped at 4°C. The cells were fixed and then treated with specific buffers for flow analysis (eBioscience, San Diego, CA). After washing three times with cold PBST buffer, 1 μg/mL goat anti-Fc receptor antibody (BD Science) was added for 10 min to prevent any non-specific binding of antibodies. The cells were washed with cold PBST three times before stepwise incubations with 1 μg/mL anti-TcdA mouse monoclonal antibody PCG-4 (GeneTex) and 1 μg/mL secondary antibody (goat anti-Fc receptor antibody) conjugated to fluorescein isothiocyanate (FITC) (Sigma-Aldrich). After the last washing step, the cells were washed with double distilled H_2O to remove the salt. The cells were simultaneously mounted onto glass, nuclei were stained with 4',6-diamidino-2-phenylindole (DAPI) (Invitrogen, Carlsbad, CA), and the preparations were stored at -20°C before confocal microscopy (Leica TCS SP5 II; Leitz, Heidelberg, Germany).

Fluorescence-activated cell sorting flow cytometry (FASC)

Vero cells seeded in T-75 flasks containing VP-SFM/4 mM glutamine were allowed to grow to 80% confluence at 37°C. An aliquot of resuspended cells (5×10^5 cells/mL) was mixed with either 80 μg/mL TcdA rRBD or its fragments at 37°C for 5 min. After washing with cold PBST, 1 μg/mL of either the anti-TcdA antibody PCG-4 or an anti-His tag antibody (AbD Serotec, Oxfordshire, UK) was added to the cells, and the mixture was incubated on ice for 30 min. After washing twice with cold PBST, 1 μg/mL FITC-conjugated secondary antibody (Sigma-Aldrich, St. Louis, MO) was added and mixed for surface staining. Before flow cytometry analysis, propidium iodide (Sigma-Aldrich) was added to assess cell viability.

Hemagglutinin activity analysis

The hemagglutinin (HA) activity assay was performed as described by Wren et al. [37]. In brief, 250 pmol of either TcdA rRBD or its fragments in a 25 μL volume was serially diluted

two-fold using PBS buffer in 96-well round-bottom plates. A suspension containing 25 μL of 2% rabbit erythrocytes rewashed with PBS to remove serum contamination was added to the wells at a 1:1 ratio. The mixtures were incubated at 4°C overnight. HA activity was calculated by visual scoring.

Surface marker and cytokine analyses for DC maturation

DC maturation analysis was performed *in vitro* as previously described [38]. C57BL/6 mice were purchased from the National Animal Center in Taiwan and held in the Animal Center of the NHRI. In brief, bone marrow-derived DCs (BMDCs) were collected from the tibiae of 6- to 8-week old C57BL/6 females. Bone marrow cells were isolated by vigorously washing with lymphocyte-conditioned medium (LCM) (RPMI 1640 containing 1% penicillin and streptomycin, 10% heat-inactivated FBS, 50 μM β-mercaptoethanol, and 50 mM HEPES) and treated with lysis buffer to remove erythrocytes. BMDCs were re-suspended at 2×10^6 cells per mL in LCM and treated with 20 ng/mL recombinant granulocyte macrophage colony stimulating factor (MoGM-CSF) (Peprotech, Rocky Hill, NJ) on days 0 and 3. An aliquot of suspended BMDCs equivalent to 2×10^6 cells/mL was seeded into 24-well plates on day 6. Different concentrations of TcdA rRBD or its fragments with or without 10 ng/mL polymyxin B were added into the wells. LPS extracted from *E. coli* O127:B8 (Sigma-Aldrich) and TcdA served as controls. After a 16- to 18-h incubation at 37°C, BMDCs were analyzed by flow cytometry (FACSCalibur, BD Biosciences, Franklin Lakes, NJ) to evaluate the up-regulation of cell surface markers. To exclude immature DCs, which represent 50% of the total cell population, the CD11c$^+$ cell population was gated for surface marker staining with specific monoclonal antibodies against CD-40, CD-80, CD-86, and MHC-II. In addition, cell culture supernatants were collected for cytokine expression. Cytokines, such as IL-6, IL-12p40 and TNF-α, were determined using specific cytokine kits purchased from eBioscience (San Diego, CA).

Circular dichroism (CD) measurement

TcdA rRBD and its fragments (F1, F2 and F3) were prepared in 10 mM phosphate buffer (pH 7.4) at a concentration of 50 μg/mL. Spectra were obtained with a J-185 spectropolarimeter (Jasco, Easton, MD) with thermal electric temperature control, and the data were acquired in continuous scanning mode with a 0.5 mm path length, a 1 nm interval and an accumulation time of 10–15 s/min. The far UV scan range was set between 260 and 200 nm with a scan speed of 50 nm/min. All data were processed using Jasco software. The background spectrum obtained with 10 mM phosphate buffer (pH 7.4) was subtracted from the acquired sample spectrum for the thermal stability test, and the temperature gradient was set between 30°C and 90°C. CD spectra were recorded at intervals of 10°C. The percent of each secondary structure was calculated from the mean residue ellipticity ($[\theta]$) according to the method suggested by the manufacturer.

Mouse immunogenicity study

BALB/c mice were purchased from the National Animal Center in Taiwan and held in the Animal Center of the NHRI. Eight groups of mice (6 BALB/c mice per group) were vaccinated with three intramuscular (IM) injections of 3, 10 and 30 μg of either TcdA rRBD or truncated fragments (F1, F2 or F3) with and without alum (AlPO$_4$) every two weeks. Before each immunization, mice were bled to collect sera, which were stored at -20°C, for anti-RBD antibody titer determination in an RBD-specific ELISA. To study the adjuvant effects of TcdA rRBD, individual groups of 6 BALB/c mice were immunized intramuscularly with 2 μg of ovalbumin (OVA) (Sigma-Aldrich) formulated with 0.3, 3 or 10 μg of either TcdA rRBD or aluminum

phosphate (AlPO$_4$) (Sigma-Aldrich). Animals that received 2 µg of OVA alone served as the controls. The mice were given three immunizations at two-week intervals and bled before each injection. Sera were collected and stored at -20°C for anti-OVA antibody titer measurement using an OVA-specific ELISA as described below.

Antigen-specific ELISA

ELISA plate wells were coated with 100 ng of either TcdA rRBD or OVA overnight and then blocked with 5% nonfat dry milk (w/v) in PBS. Mouse antisera serially diluted 2-fold with PBS containing 1% BSA (Calbiochem, Darmstadt, Germany) were added to the wells, followed by incubation at room temperature (RT) for 2 h. Each group of pre-immunized serum was diluted fifty-fold with PBS. After washing three times with PBST, 50 ng/mL of either anti-IgG isotypes (Invitrogen, Carlsbad, CA) or anti-IgA (Invitrogen, Carlsbad, CA) HRP-conjugated IgG (KPL, Gaithersburg, MD)-specific antibodies diluted in PBS containing 1% BSA was added to the wells and incubated at RT for 1 h. After washing three times with PBST, the plates were treated with TMB peroxidase substrate (KPL) at RT in the dark for 20 min. To determine the anti-RBD or anti-OVA titers, the OD$_{450\ nm}$ absorbance was measured using a spectrophotometer.

Anti-toxin neutralization assay

The anti-TcdA neutralization assay was performed according to the protocol previously described by Seregin *et al.* [23]. Briefly, Vero cells (2×10^4 per well) were seeded into 96-well plates containing VP-SFM culture medium and 4 mM glutamine at 37°C, and the cells were allowed to grow to confluence. Mouse sera from mice immunized either with TcdA rRBD or truncated fragments with and without alum were serially diluted two-fold with fresh VP-SFM, mixed with an equal volume of 20 ng/mL TcdA from *C. difficile* VPI 10463 (The Native Antigen Company Ltd, Oxfordshire, UK) and incubated at room temperature for 1 h. The mixture was added to the 96-well plates containing Vero cells and incubated at 37°C for 24 h. Anti-toxin neutralization titers were calculated as the highest serum dilution that could protect 50% of the cells from rounding due to toxin cytotoxicity. Cellular toxicity was recorded using a microscope equipped with a camera.

Toxin A challenge mouse model

A lethal TcdA challenge mouse model was established to assess the efficacy of anti-RBD immune responses *in vivo* using the protocol previously described by Seregin et al. [23]. Briefly, 4 groups of BALB/c mice (10 mice per group) were immunized IM with either PBS or three dosages of TcdA rRBD (0.3, 3, and 30 µg) at days 0, 14, and 28. After three immunizations, mice were challenged with 150 ng of TcdA from *C. difficile* VPI 10463 (5× lethal dose (LD$_{50}$)) (The Native Antigen Company) by intra-peritoneal injection at day 35, and the survival rate was monitored for 14 days. The mice were observed twice daily during the first 3 days.

Statistical analysis

The data were expressed using Prism 5 version 5.01 (GraphPad Software, Inc.). The antibody titers are displayed as the mean±SEM from the experiments. Significant differences were analyzed using a two-tailed Student's t-test comparing the means obtained for each treatment with the control group. A *p*-value of <0.05 was considered significant.

Results

Design of the consensus sequence of RBD

Based on previous studies [8, 22, 24, 29–30], the receptor-binding domain of TcdA is located between residues 1800 and 2710 in its C-terminal region and has a molecular size of approximately 100 kDa. Amino acid sequences of TcdA RBD from different *C. difficile* isolates deposited in the NCBI protein database were aligned and examined. The results indicated that the TcdA RBD amino acid sequence was highly conserved with 97% identity. Moreover, the amino acid sequences of the RBDs from different *C. difficile* isolates could be divided into two groups. One group was biased to strains including VPI 10463 and ATCC9689, which are the reference strains for *C. difficile* toxin studies, and the other group included the majority of PCR-ribotype 027 isolates. In this study, the selected consensus amino acid sequence of RBD was composed of 911 residues and was identical to that of BI/NAP1/027-related isolates, as expected because the majority of the protein sequences deposited in the NCBI database are ribotype 027 strains (Fig 1A). The differences between the amino acids of the consensus sequence and the VPI 10463 reference strain are highlighted in Fig 1A. There are 33 synonymous changes within the RBD, including 11, 24 and 16 amino acids that differ in the F1, F2 and F3 fragments, respectively. In addition, 12 changes were found within the 7 potential lectin-binding sites. These differences affected the cell-binding activities of these fragments and influenced the quality of the antibodies generated in the animal immunogenicity studies (see below). Upon further sequence analysis, the consensus sequence contained 34 short repeat units containing 18 to 22 amino acids (Fig 1B). Previous studies by Dove *et al.* [30] and Ho *et al.* [31] suggested that the RBD contained 38 and 32 short repeat units, respectively. This discrepancy in the estimated number of repetitive sequences may be the result of using different analysis software programs.

To study the specific roles and functions of the 7 putative receptor-binding regions, TcdA RBD was divided into three fragments, F1, F2 and F3, which correspond to the N-terminal residues 1 to 411, the middle region residues 296 to 701, and the C-terminal residues 524 to 911 of TcdA RBD, respectively (Fig 1C). Each fragment was purposely designed to contain 3 potential lectin-like (oligosaccharide) receptor-binding (LR) sites. F1 and F2 contain an overlapping LR site #3; F2 and F3 have an overlapping LR site #5 (Fig 1C).

Production of recombinant RBD (rRBD) and its fragments

The DNA coding sequence of the tcdA RBD was designed employing codon usage optimization, synthesized, inserted into the pET-22b vector and successfully expressed in *E. coli* as shown in Fig 2. After a single-step purification using Ni-affinity chromatography, highly purified TcdA rRBD was obtained, and its purity was analyzed by SDS-PAGE to be >95% (Fig 2A); trace amounts of TcdA rRBD degradation fragments were detected using a TcdA-specific antibody by western blot analysis (Fig 2B). These degradation products are likely the result of proteolytic digestion during the purification process [39]. In any event, at least 20 mg of highly enriched TcdA rRBD (Fig 2B, lane 4) was easily obtained from 1 L of bacterial culture. Most of the *E. coli* endotoxin (LPS) was successfully removed by passing the TcdA rRBD preparation through an E membrane; the residual LPS in the purified TcdA rRBD was found to be below 30 EU per mL based on the LAL assay. Although a simple and rapid method for producing TcdA rRBD with high purity was successfully developed, TcdA rRBD was found to be unstable and easily lost its biological function during the freeze-thaw process (see below). We found that the best conditions for preserving TcdA rRBD integrity were to store the protein at 3 to 5 mg/mL in PBS containing 10% (v/v) glycerol at -80°C.
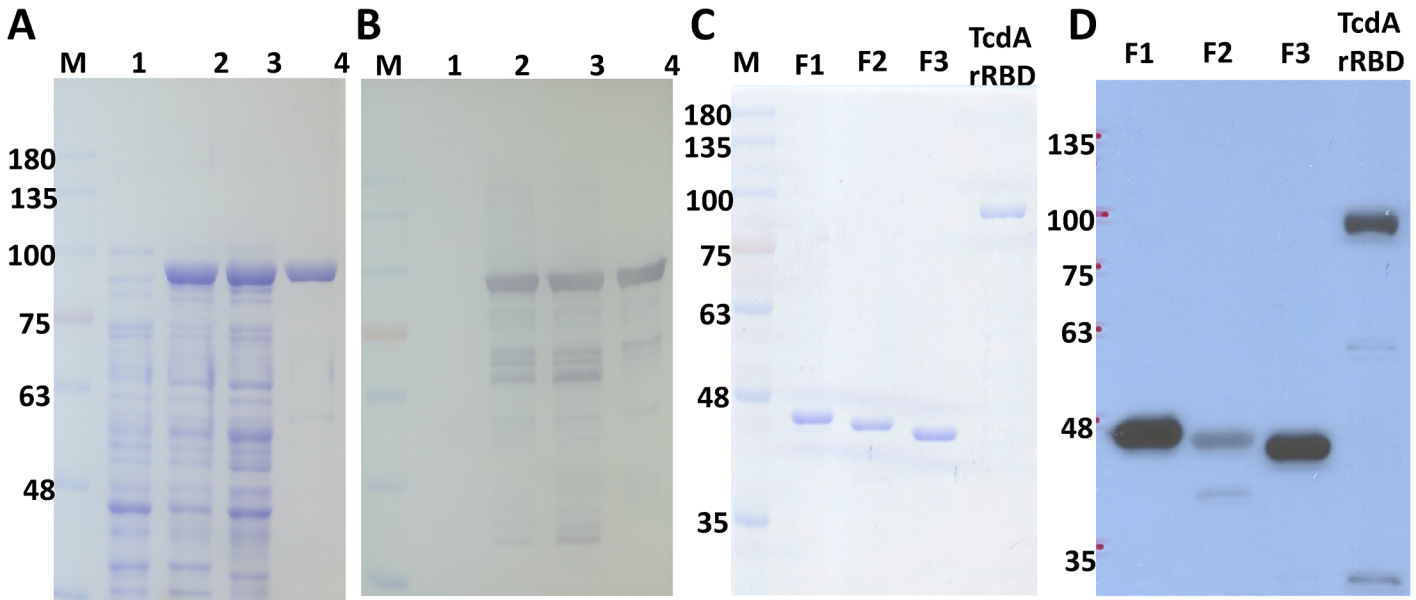
Fig 2. The biochemical characterization of recombinant _C. difficile_ TcdA rRBD. TcdA rRBD and its truncated fragments with the consensus sequence expressed in the _E. coli_ JM109 strain. The expression and purification of TcdA rRBD were confirmed by SDS-PAGE (A) and western blot with a toxin A-specific monoclonal antibody (B); lanes 1 to 4 represent non-induction, induction, crude lysate, and chromatographic purified samples, respectively. The purity of TcdA rRBD fragments F1, F2 and F3 was confirmed by SDS-PAGE (C) and western blot with a toxin A-specific monoclonal antibody (D).

doi:10.1371/journal.pone.0135045.g002

Using the same rapid purification method, highly purified F1 (25 mg), F2 (15 mg) and F3 (50 mg) fragments of TcdA rRBD were successfully obtained from 1 L of bacterial culture. The purity was >97%, as analyzed by SDS-PAGE (Fig 2C) and western blot analysis using a TcdA-specific monoclonal antibody (Fig 2D). The residual LPS in the purified F1, F2 and F3 preps were all <10 EU per mg of protein based on the LAL assay. These recombinant RBD fragments were also stored in PBS containing 10% (v/v) glycerol at -80°C. F1 and F3 had the same solubility as TcdA rRBD (>3 mg/mL), but F2 was less soluble and was stored at <1 mg/mL. As shown in Fig 2D, F2 was not well recognized by the anti-TcdA monoclonal antibody PCG-4, which was generated from the VPI 10463 strain. This lower antigenicity may be attributable to the 24 amino acid changes in F2 compared to those in the VPI 10463 strain (Fig 1A).

Biological characterization of rRBD and its fragments

CD secondary structure analysis of TcdA rRBD and its fragments was performed to confirm that the proteins were correctly folded to form a majority β-sheet structure (>43%) (S1A Fig). The results are consistent with other reports indicating that the fragments of RBD containing 5 to 15 short repetitive sequences could form stable folded β-solenoid secondary structures independent of other functional domains in the TcdA [31–32]. In addition, the thermal stability of each recombinant protein was determined, and the melting temperatures (Tm) for TcdA rRBD, F1, F2 and F3 were found to be 48.5, 43.8, 47.3 and 51.5°C, respectively (S1B Fig).

The hemagglutinin activity of TcdA rRBD was evaluated using rabbit erythrocytes. TcdA rRBD could agglutinate rabbit erythrocytes at concentrations as low as 0.4 pmol (Fig 3A) and was more potent than TcdA (1.6 pmol). The biological function (HA activity and binding to Vero cells) of TcdA rRBD correlates with its active conformation because freeze-thaw and/or boiling processes either reduced or eliminated these biological properties. Therefore, preserving the functionally active conformation of TcdA rRBD is very important; however, it is easily
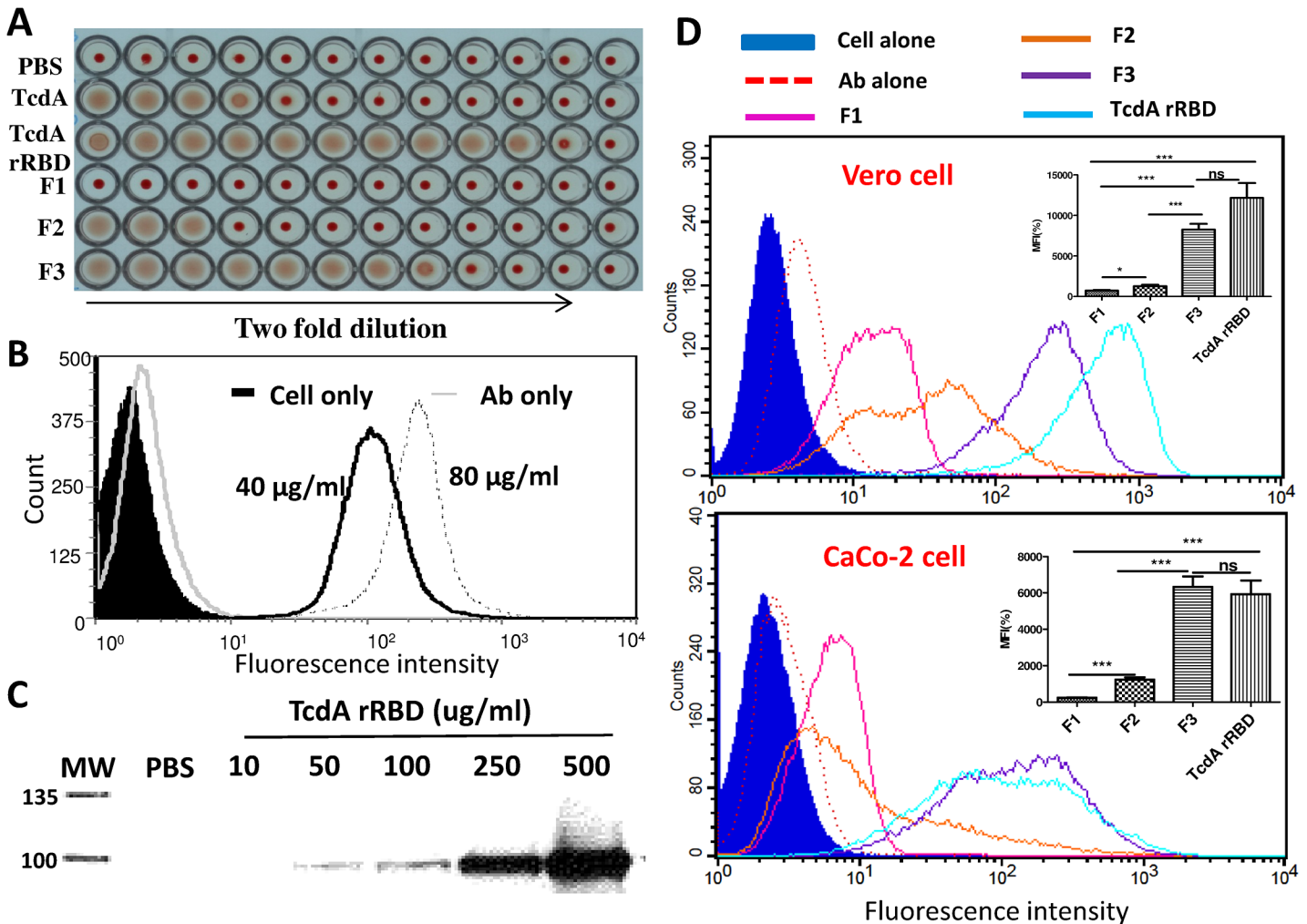
Fig 3. Several functional assays were used to evaluate the biological properties of TcdA rRBD and its fragments. (A) A hemagglutinin (HA) assay was performed starting with either 15 pmol of TcdA or 250 pmol of TcdA rRBD, F1, F2 and F3 mixed with 2% rabbit erythrocytes in a 1-to-1 ratio (v/v). TcdA rRBD cell-binding ability was characterized by flow cytometry (B) and western blot (C) using an anti-TcdA specific monoclonal antibody. Different amounts of TcdA rRBD were used to treat cells to evaluate binding ability in a dose-dependent manner. (D) Vero and Caco-2 cell-binding abilities of TcdA rRBD and its fragments (1 μM) were characterized by FACS analysis as described in the Materials and Methods. The MFI from TcdA rRBD fragment binding assays were measured to evaluate statistical significance, as shown in the bar charts within the FACS figures. The symbols *, ** and *** indicate $p<0.05$, $p<0.01$ and $p<0.005$, respectively.

doi:10.1371/journal.pone.0135045.g003

influenced by purification and storage conditions. Together, these results indicate that the purified TcdA rRBD is correctly folded and exhibits functions similar to those of the receptor-binding domain of native toxin A.

To investigate whether TcdA rRBD fragments possess hemagglutinin activity, F1, F2 and F3 were evaluated for HA activity using rabbit erythrocytes. As shown in Fig 3A, F3 had similar HA activity to TcdA (2 pmol), while F2 (32 pmol) had much lower HA activity (p<0.01). Surprisingly, F1 did not agglutinate rabbit erythrocytes even at protein concentrations as high as 1 μmol (Fig 3A). However, the β-sheet secondary structure revealed by the CD spectra analysis indicated that the purified F1 folded correctly (S1 Fig).

To confirm the biological function of TcdA rRBD, Vero cell-binding activity was analyzed by western blot and flow cytometry. The results shown in Fig 3B indicate that 0.4 μM (40 μg/mL) TcdA rRBD was unambiguously bound to the Vero cell surface, as detected by FACS

analysis. We also demonstrated that TcdA rRBD was able to recognize and strongly bind to Vero cells in a dose-dependent manner, as assessed by both FACS and western blot analyses (Fig 3B and 3C). The binding of TcdA rRBD fragments to Vero cells was tested using FACS analysis. At 1 µM protein concentration, F3 had the highest fluorescence intensity, as shown in Fig 3D. F1 had the lowest binding and fluorescence intensity compared to TcdA rRBD and F3. F2 had bi-phasic binding activity to Vero cells, indicating that F2 binds to at least two types of receptors. As shown in Fig 2D, the TcdA-specific monoclonal antibody recognized F2 least; thus, to eliminate the reduced antibody binding affinity, FACS analyses were repeated with an anti-His tag antibody, and similar results were obtained (data not shown). This result confirmed that the binding activity to Vero cells was as follows: TcdA rRBD>F3>F2>F1 ($p<0.001$). To further show the sensitivity of Vero cell binding, different concentrations of TcdA rRBD and its fragments were tested. Under the current binding assay conditions, the minimum concentration required to induce a 3-fold increase in fluorescence intensity compared to the negative control (ovalbumin) for TcdA rRBD, F1, F2 and F3 bound to Vero cells was 10, 50, 500, and 10 nM, respectively.

The binding of TcdA rRBD and its truncated fragments to Caco-2 cells was also evaluated using FACS analysis. At the 1 µM protein concentration, TcdA rRBD and F3 exhibited the highest binding and fluorescence intensity to Caco-2 cells, as shown in Fig 3D, but the bi-phasic fluorescence intensity suggested that both rRBD and F3 could bind at least two types of receptors. F1 and F2 exhibited lower binding and fluorescence intensity compared to TcdA rRBD and F3. F2 also showed multi-phasic binding activity to Caco-2 cells, indicating that F2 binds to more than two types of receptors. As shown in Fig 3D, the current results indicate that the binding activity to Caco-2 cells was as follows: F3≥TcdA rRBD>F2≥F1 ($p<0.001$).

The binding affinity and kinetics of TcdA rRBD and its fragments to Vero cells were further analyzed, and the apparent K_d (defined as the half-maximal binding to the receptors) for TcdA rRBD was 0.14 µM (Fig 4A). The results from the fragment cell-binding studies indicate the apparent K_d values to be 0.26, 0.56 and 0.16 µM for F1, F2 and F3, respectively (Fig 4A). TcdA rRBD and F3 quickly bound to certain receptor(s) on the surface of Vero cells, and >8 µM TcdA rRBD and F3 were required to saturate all receptors (Fig 4A). In contrast, the binding of F1 to its receptor(s) was rapid and saturated at 2 µM. These results suggest that F3 and TcdA rRBD have similar binding activities but may have different binding specificities and sensitivities compared to F1.

The binding assay was also performed with Caco-2 cells, and the apparent K_d was 0.09 µM for TcdA rRBD, which was similar to that obtained from the Vero cell studies (Fig 4B). The apparent K_d values were 0.18, 0.32 and 0.08 µM for F1, F2 and F3, respectively (Fig 4B). F3, similar to TcdA rRBD, binds to Caco-2 cells much stronger and more rapidly than F1 and F2 ($p<0.001$). All cell binding was easily saturated at 1 µM (Fig 4B). These results show that TcdA rRBD and F3 have similar binding specificities and sensitivities to Vero and Caco-2 cells but differ from F1.

To optimize the protein concentration used for the identification of surface receptor(s) in Vero cells, F1 cell binding was analyzed by immunoblot. F1 bound strongly to Vero cells in a dose-dependent manner, as analyzed by immunoblotting (S2 Fig). In the same assay, both F2 and F3 exhibited less binding than F1 (S2 Fig). These immunoblot results are inconsistent with those obtained from flow cytometry, in which F3 demonstrated significantly better binding ($p<0.001$) than F1 to the receptor(s) on the surface of Vero cells (Fig 3D). This discrepancy could be attributable to the 30-min cell binding incubation time, in which most F3 translocated into the cytosol but F1 remained bound to the receptor on the cell surface (see the cellular uptake of TcdA rRBD and its fragment below). Therefore, much less F3 was observed in the immunoblot analysis of cell membrane lysates. Preliminary results indicate that 30 to 60 µg of
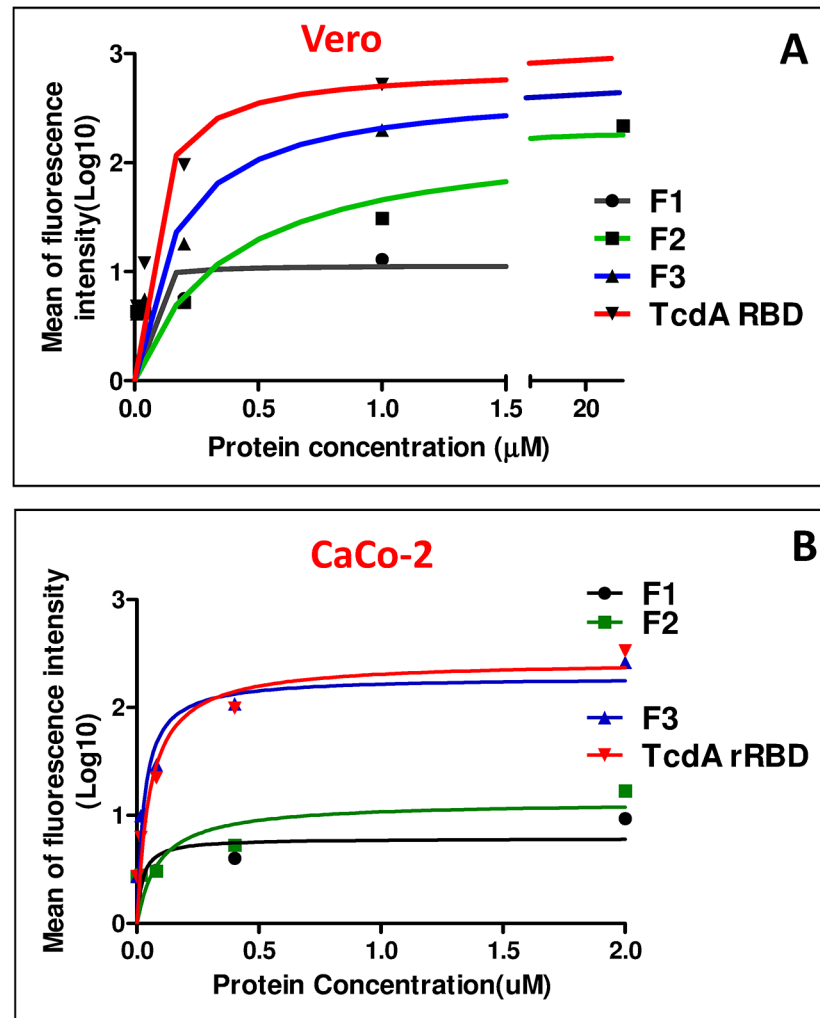
Fig 4. Cell-binding affinities and kinetics of TcdA rRBD and its fragments were determined by FACS analysis as described in the Materials and Methods.

doi:10.1371/journal.pone.0135045.g004

F1 are sufficient to form strong complexes with the cell receptors, which could be pulled down with the anti-TcdA monoclonal antibody (Huang *et al.*, unpublished result).

Cellular uptake of TcdA rRBD and its fragments

C. difficile toxin binding to cell surfaces promotes its cellular internalization through receptor-mediated clathrin-dependent endocytosis [40–41]. To verify whether TcdA rRBD exhibits this biological activity, a Vero cell-binding assay was performed *in vitro*, and TcdA rRBD binding was analyzed by flow cytometry. After TcdA rRBD binding, the specific immunofluorescence signal against TcdA rRBD decreased with time (Fig 5A). These decreases in fluorescence signal intensity suggest that TcdA rRBD could either be internalized into the cytosol from the surface or degraded. Therefore, confocal immunofluorescence assays were performed to localize TcdA rRBD after binding to Vero cells. The results indicate that the cellular uptake of TcdA rRBD occurs very quickly (Fig 5B). The cell surface-binding and internalization processes of TcdA rRBD were observed after 5 min of incubation, as illustrated by strong anti-rRBD fluorescence signals around the cell surface. After 15 min of incubation, the majority of TcdA rRBD had
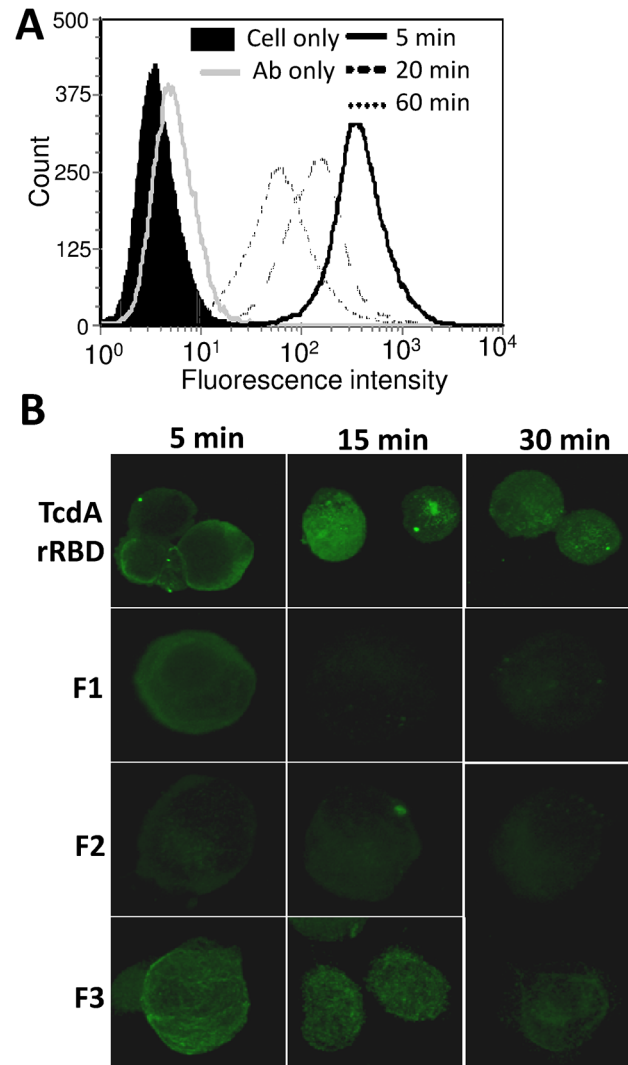
Fig 5. Cellular uptake of TcdA rRBD and its fragments. (A) TcdA rRBD binding signals on the surface of Vero cells were detected by flow cytometry after TcdA rRBD inoculation at the indicated times. (B) The internalization signals of TcdA rRBD and its fragments in Vero cells were evaluated by confocal microscopy at 5, 15, and 30 min. The images were collected from a single stack in the central region of the z-axis. Green fluorescence signals represent the locations of TcdA rRBD, F1, F2 and F3.

doi:10.1371/journal.pone.0135045.g005

entered the cytosol, as indicated by very strong confocal immunofluorescence signals (Fig 5B). After 30 min, a decrease in the immunofluorescence signal was noted and was likely attributable to lysosomal degradation (Fig 5B). These trends support the notion that TcdA rRBD binds specifically to the cell surface, is internalized into the cytosol, and is cleaved into fragments by lysosomal degradation. Due to its rapid internalization process, rRBD could potentially serve as a carrier for drug delivery systems.

Because F1, F2 and F3 are all capable of binding to Vero cells, it is of interest to determine whether they would be internalized into the cytosol after binding to the cell receptor(s). As illustrated by immunofluorescence signals in the confocal studies, cell surface binding and internalization processes were observed for F2 and F3 after 15 and 5 min of incubation, respectively (Fig 5B). After 15 min of incubation, strong confocal immunofluorescence signals suggested that F3 entered the cytosol. Similar to TcdA rRBD, a decrease in the

immunofluorescence signal was observed after 30 min of incubation (Fig 5B). These findings support the notion that F3 specifically binds to the cell surface, is internalized into the cytosol, and is cleaved into fragments by lysosomal degradation. After a 15-min incubation, F2 exhibited weak confocal immunofluorescence signals, which suggested that some F2 entered the cytosol (Fig 5B). Conversely, after 30 min of incubation (and even after 75 min), F1 exhibited very weak confocal immunofluorescence signals, which suggested that little F1 entered the cytosol (Fig 5B). To confirm that the cellular uptake was receptor-mediated clathrin-dependent endocytosis, chlorpromazine (CPZ) was used and found to inhibit TcdA rRBD and F3 internalization, as shown in S3 Fig. Based on the results obtained from the cell-binding studies, HA assay and cellular uptake studies, the putative receptor-binding domains in F1, F2, and F3 likely play different and specific biological roles and functions.

Dendritic cell maturation triggered by TcdA rRBD

C. difficile toxin A has been reported to up-regulate cell surface marker expression and cytokine secretion from dendritic cells [42]. In addition, previous studies [43–44] have reported that the C-terminal part of TcdA could serve as a mucosal adjuvant to enhance the immune response toward a co-administered antigen. Therefore, TcdA rRBD was tested for its ability to promote the maturation of DCs. BMDCs from C57BL/6 mice were treated with increasing amounts (0.3 to 10 µg) of TcdA rRBD. Cell surface biomarkers associated with DC maturation (CD-40, CD-80, CD-86, and MHC-II) and the secretion of pro-inflammatory cytokines (IL-6, IL12, and TNF-α) were examined using FACS analysis and cytokine-specific ELISA, respectively. To preclude the interference of LPS contamination, TcdA rRBD samples used in the current studies had very little LPS contamination (0.03 EU/µg of protein). In addition, polymyxin B was added to the DC samples to prevent activation by LPS through the Toll-like receptor 4 pathway. Surface biomarkers of DC maturation were up-regulated, and the production of pro-inflammatory cytokines (IL-6, IL12, and TNF-α) increased in a dose-dependent manner from 0.5 to 6 µM (data not shown). A 2-µM TcdA rRBD concentration in the final assay solution was selected for subsequent analyses. Both DC maturation biomarkers were up-regulated (Fig 6A to 6D), and a significant increase in the production of pro-inflammatory cytokines (IL-6, IL12, and TNF-α) was detected in TcdA rRBD-treated BMDC culture supernatant (Fig 7A to 7C). The results were not influenced by minor LPS contamination, as there was no significant difference between polymyxin B-treated and non-treated samples, as shown in Figs 6 and 7. We boiled both TcdA rRBD samples and LPS to denature and destroy their biological functions. Boiling did not affect LPS-induced DC activation but fully abolished TcdA rRBD-mediated DC activation. Overall, this result clearly demonstrates that DC activation is mediated by TcdA rRBD.

To assess whether the fragments of TcdA rRBD have similar adjuvant properties to TcdA rRBD, both DC maturation biomarker and the production of pro-inflammatory cytokine (IL-6, IL12, and TNF-α) assays were performed with 2 µM of F1, F2 or F3 with and without polymyxin B. DC biomarkers and the production of pro-inflammatory cytokines were up-regulated and increased in BMDC culture (Figs 6 and 7). Interestingly, as shown in Figs 6 and 7, F1 and F2 were less effective (p<0.01) in inducing DC maturation biomarkers and the production of pro-inflammatory cytokines (IL-6, IL12, and TNF-α) compared to cells treated with either TcdA rRBD or F3. These results are consistent with previous reports [42–44] and suggest that TcdA rRBD and F3 are potential candidates for recombinant subunit vaccine development against CDI and can be used as potent adjuvants to enhance immune responses against weak immunogens (see below).
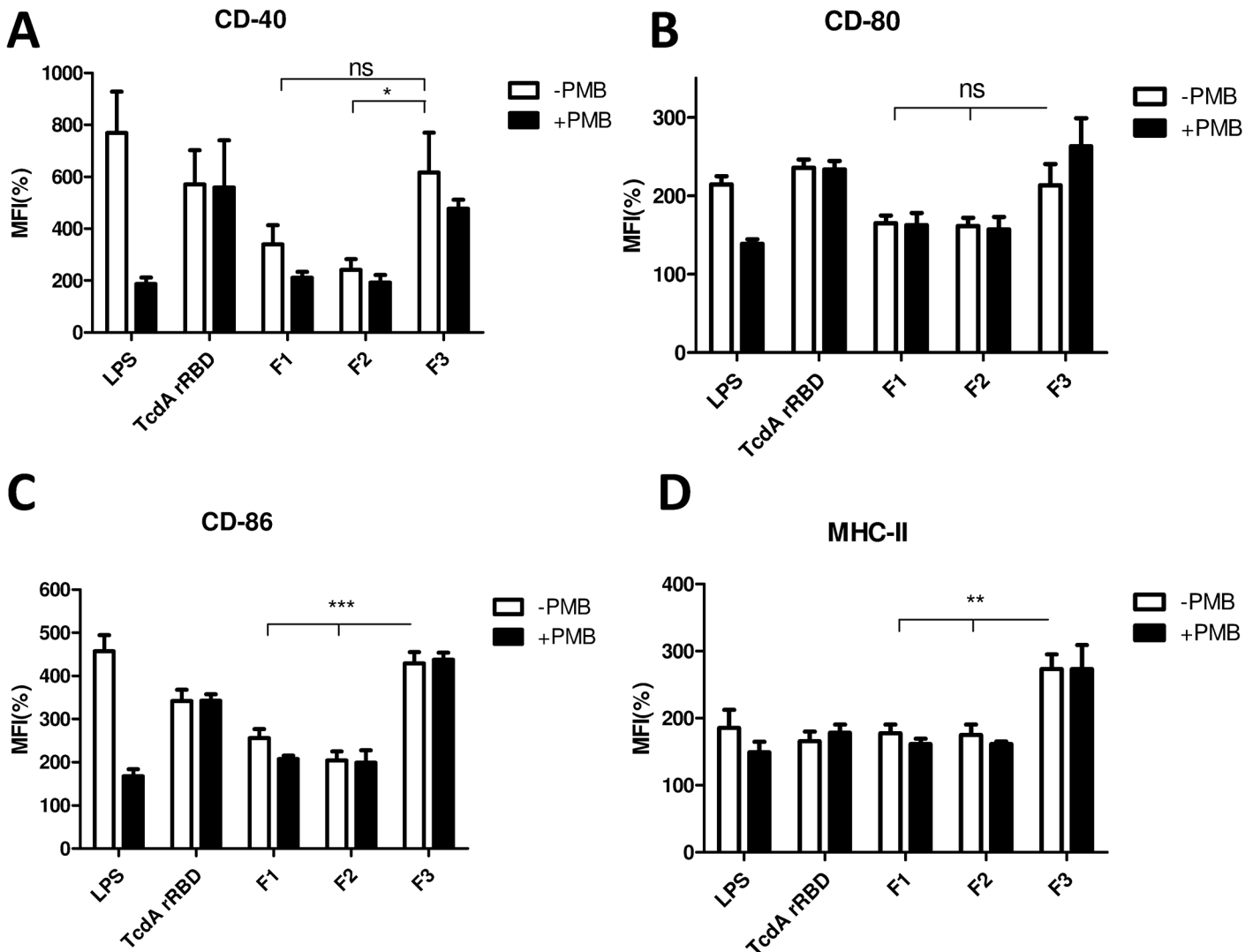
Fig 6. Up-regulation of surface biomarkers of BMDCs by either TcdA rRBD or its truncated fragments. BMDCs from C57BL/6 were collected and treated with GM-CSF at days 0 and 3. TcdA rRBD was added at day 6 for 18 h, and then, DCs were collected to analyze their surface markers, including CD40 (A), CD80 (B), CD86 (C), and MHC II (D), by flow cytometry. All groups were divided as polymyxin B-treated (PMB) (black-net bar) or non-treated (gray-net bar) to exclude LPS contamination. All surface marker signaling was normalized by calculating the ratio of mean fluorescence intensity (MFI) between the medium control and treatments. The symbols *, ** and ns indicate $p < 0.05$, $p < 0.01$ and no significant difference, respectively.

doi:10.1371/journal.pone.0135045.g006

Mouse immunogenicity studies

To assess the immunogenicity of TcdA rRBD, groups of mice were vaccinated with either TcdA rRBD alone or formulated with alum (AlPO4). Analyses of antisera from mice immunized with varying doses of TcdA rRBD using a RBD-specific ELISA revealed that TcdA rRBD alone could induce significant antibody responses (S4A Fig). The results from the current mouse immunogenicity studies indicate that TcdA rRBD is highly immunogenic because mice vaccinated twice with 3 μg of TcdA rRBD alone produced very strong anti-rRBD IgG antibodies with a titer of $>10^4$ (week 4 in S4A Fig). Moreover, in antisera from mice vaccinated 3 times with TcdA rRBD, both IgG_1 and IgG_2 isotype antibody responses were observed (S4B Fig). Systemic IgA antibody responses were also elicited by TcdA rRBD vaccination (S4B Fig). The pre-immunized mouse sera and/or sera from mouse immunized with PBS served as
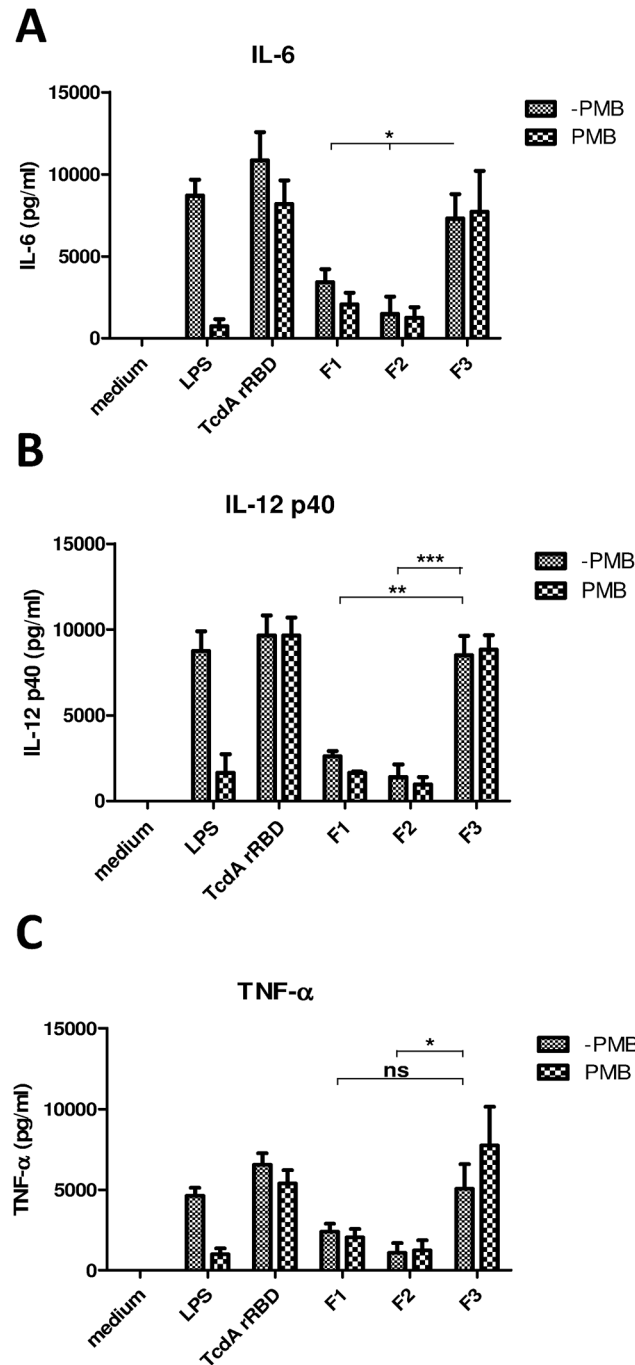
Fig 7. Cytokine secretion from BMDCs treated with TcdA rRBD or its truncated fragments. After BMDCs were treated with TcdA rRBD or its truncated fragments at day 6 for 18 h, the culture supernatants were collected and analyzed for cytokine profiles using specific cytokine ELISAs: (A) IL-6, (B) IL12p40, and (C) TNF- α. The symbols * and ** indicate $p<0.05$ and $p<0.01$, respectively.

controls, and no anti-RBD IgA antibody signal was detected at fifty-fold dilution. At 6 weeks post-vaccination, the anti-rRBD IgG antibody titers (~ 1×10^5) elicited by 3 μg of TcdA rRBD alone were not different from those obtained with either 3×10 μg of TcdA rRBD formulated with alum or 3×10 μg of TcdA toxoid (S4A Fig and Table 1). These results clearly indicate

Table 1. *C. difficile* toxin A neutralization titers of antisera from groups of 6 mice immunized 3 times with varying amounts of either TcdA rRBD or its fragments formulated with or without alum.

Mice immunized with		Anti-rRBDIgG titers[a]	Neutralization titers[b]	Protection rate (%)[c]
TcdA rRBD	0 µg	<100	<4	0
	3 µg	9.3×10^4	32	16
	10 µg	1.7×10^5	256	ND
	30 µg	5.3×10^4	128	67
	10 µg + alum	1.2×10^5	128	83
RBD F1	10 µg	1.7×10^4	8	ND
	10 µg + alum	1.5×10^6	64	50
RBD F2	10 µg	6.7×10^3	4	ND
	10 µg + alum	6.5×10^4	16	0
RBD F3	10 µg	1.1×10^4	16	ND
	10 µg + alum	8.1×10^4	64	50
TcdA toxoid[d]	10 µg	7.7×10^4	256	ND
	10 µg + alum	3.7×10^5	2048	100

[a] The titers were obtained from sera pooled from 6 mice.

[b] The neutralization titer against toxins was defined as the highest sample dilution that could prevent 50% of cell rounding induced by toxins.

[c] Groups of 6 mice were immunized 3 times with 10 µg of different RBD proteins formulated with or without alum and then challenged with $5 \times LD_{50}$ of toxin A. The survival rate in each group was reported at 36 h post-challenge.

[d] A group of 6 mice was immunized 3 times with 10 µg of TcdA toxoid formulated with or without alum.

ND indicates not performed.

doi:10.1371/journal.pone.0135045.t001

that 3 µg of TcdA rRBD can induce strong anti-rRBD IgG antibody responses. The anti-rRBD IgG antibody titers ($\sim 1 \times 10^5$) could be the maximal antibody responses elicited by TcdA rRBD because 30 µg of TcdA rRBD did not enhance the titer (5×10^4) (S4A Fig and Table 1).

When mouse immunogenicity was assessed with each RBD fragment, the 6-week post-vaccination anti-RBD IgG antibody titers ($\sim 1 \times 10^4$) elicited by 10 µg of either F1 or F3 were not different from those obtained with 10 µg of TcdA rRBD (Fig 8). Antisera from mice vaccinated three times with 10 µg of F2 had lower levels of anti-rRBD IgG antibodies compared with those obtained from either F1 ($p<0.01$) or F3 ($p<0.05$). Interestingly, anti-rRBD IgG antibody titers were enhanced by 5- to 10-fold when the RBD fragments were formulated with alum, but that result was not observed with 3×10 µg of TcdA rRBD formulated with alum (S5 Fig and Table 1). As shown in S5 Fig, alum formulated with F1 elicited the strongest anti-RBD antibody responses compared to those obtained from alum formulated with either F2 ($p<0.001$) or F3 ($p<0.01$).

Immunological characterization of anti-rRBD sera

To test whether mouse anti-RBD antibodies elicited by TcdA rRBD could functionally neutralize the cytotoxicity of TcdA, antisera were evaluated in a Vero cell cytotoxicity assay as described in the **Materials and Methods**. As shown in Table 1, antisera from mice immunized with 10 µg of TcdA rRBD were found to have a neutralization titer (NT) equal to 256 that prevents 50% of the cell death resulting from toxin A cytotoxicity. The neutralization titers obtained from mice immunized with 3×10 µg of TcdA rRBD formulated with alum were insignificant compared to those obtained from TcdA rRBD alone (Table 1). Surprisingly, the mouse neutralization titer (NT = 128) obtained with 30 µg of rRBD without adjuvant was comparable to titers elicited by 10 µg of TcdA rRBD alone (NT = 256) or formulated with alum
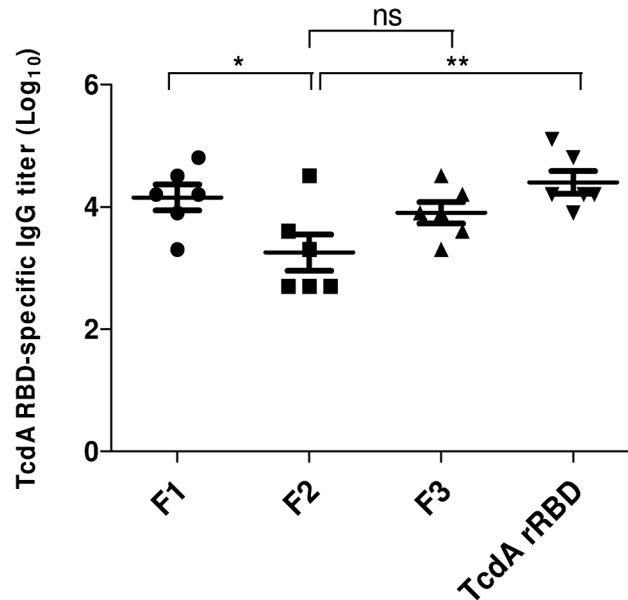
Fig 8. The immunogenicity of TcdA rRBD and its truncated fragments in mice. BALB/c mouse anti-RBD antibody responses elicited by 3×10 μg of either TcdA rRBD or its fragments. Anti-RBD IgG titers at 6 weeks were determined by RBD-specific ELISA.

(NT = 128) or 10 μg of TcdA toxoid alone (NT = 256) ([Table 1]). In contrast, the highest anti-TcdA NT was obtained from mice immunized with 3×10 μg of TcdA toxoid formulated with alum (NT = 2048). The current results indicate that 10 μg of TcdA rRBD alone could induce significant functional neutralizing antibody levels against TcdA. The anti-RBD IgG antibody responses elicited by freeze-thaw or heat-treated rRBD were significantly lower and exhibited no neutralizing activity (data not shown). Thus, preserving the functionally active conformation of TcdA rRBD is very important.

To test whether antisera obtained from mice vaccinated 3 times with 10 μg of F1, F2 or F3 alone could functionally neutralize the cytotoxicity of TcdA, antisera were assessed in the Vero cell cytotoxicity assay and had low NT (NT = 8, 4 and 16 for F1, F2 and F3, respectively) ([Table 1]). In contrast, the neutralization titers were significantly ($p<0.05$) increased (at least 4-fold) when the mice were immunized with RBD fragments formulated with alum ([Table 1]).

To further evaluate the role of this anti-toxin neutralizing activity *in vivo*, mice were immunized 3 times with increasing doses of TcdA rRBD (0.3, 3, or 30 μg) and challenged 5 times with the lethal dose 50 (LD_{50}) of toxin A ([Fig 9A]). A low dose vaccination (0.3 μg) induced good anti-RBD antibody responses (titer = 3×10^3) that were not protective ([Fig 9A]), although NT = 8 was identified in the pooled sera. The sera obtained from mice vaccinated with 3 and 30 μg of TcdA rRBD had NT = 32 and 128, respectively, but their protection rates were 17% and 67%, respectively ([Fig 9A] and [Table 1]). When mice vaccinated with 10 μg of F1, F2 or F3 formulated with alum were challenged with $5 \times LD_{50}$ of TcdA, the survival rates were 50%, 0%, and 50% for the F1, F2 and F3 groups, respectively ([Fig 9B]). This 50% protection rate may be attributable to strong neutralizing antibody responses (NT = 64) induced by F1 and F3 formulated in alum, whereas the neutralizing antibody responses induced by F2 formulated in alum remained low (NT = 16) and provided no protection ([Table 1]). Interestingly, mice immunized with 10 μg of TcdA rRBD formulated with alum demonstrated 83% protection against a TcdA challenge, and the neutralization titer was 128. Taken together, the present results suggest that protective immune responses are correlated with anti-toxin neutralization titers ([Table 1]). As
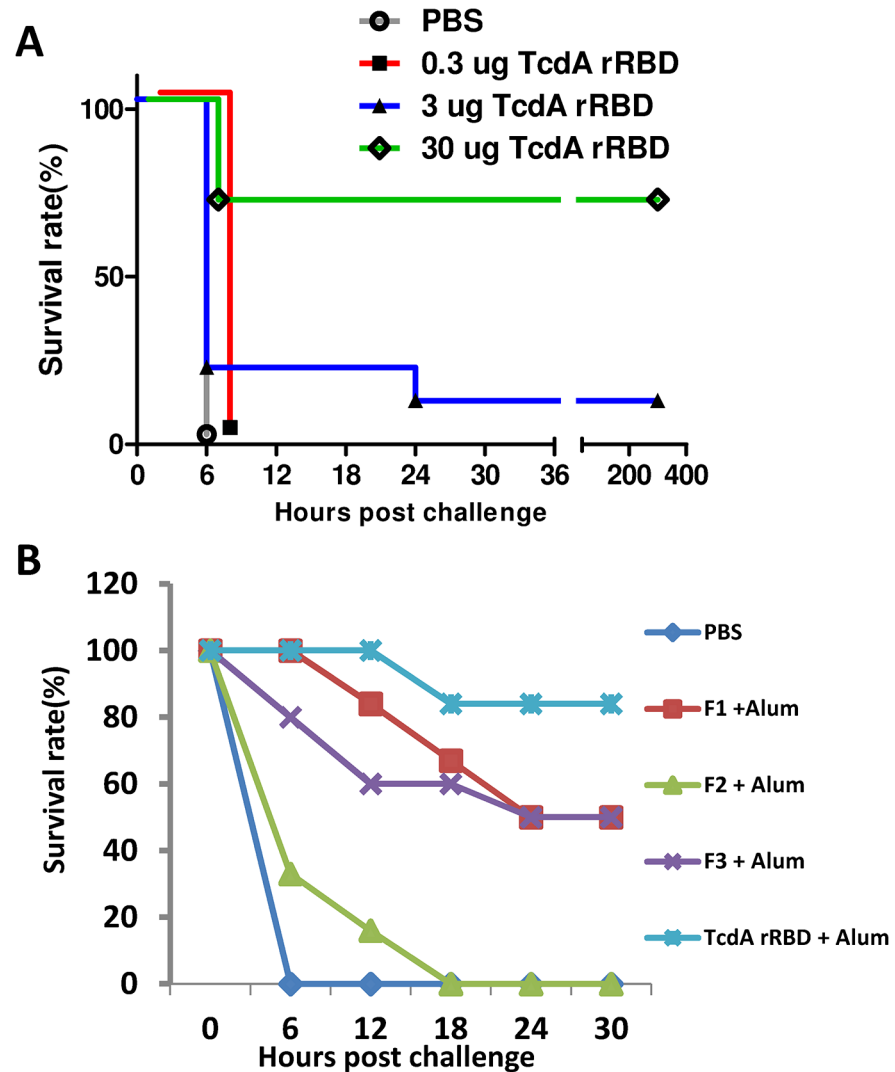
Fig 9. Protection of TcdA rRBD against lethal toxin A challenge. (A) BALB/c mice were challenged with a lethal dose of toxin A two weeks after three immunizations with TcdA rRBD (0.3, 3, and 30 μg) via intramuscular injection. (B) BALB/c mice were challenged with a lethal dose of toxin A two weeks after 3 × 10 μg of PBS, TcdA rRBD, or F1, F2 or F3 formulated with alum by intramuscular injection. The survival rate is reported at the defined time.

doi:10.1371/journal.pone.0135045.g009

TcdA rRBD, F1 and F3 formulated with alum can elicit strong immune protective responses against *C. difficile* toxin A, they should be considered as components in CDI subunit vaccines.

Adjuvant properties of TcdA rRBD and its fragments

Previous studies [43–44] have reported that the C-terminal part of TcdA could serve as a mucosal adjuvant to enhance the immune response toward a co-administered antigen, and the present study also demonstrated that TcdA rRBD is capable of promoting the maturation of dendritic cells and inducing strong functional antibody responses; these factors prompted us to investigate whether TcdA rRBD and its fragments could be used as an adjuvant. A ten-fold increase in anti-OVA IgG titers (~1×10^4) was observed in the mouse group immunized with OVA (2 μg) formulated with TcdA rRBD (10 μg) compared to titers obtained with OVA alone

([Fig 10A](#)). The mouse immunogenicity studies were repeated with OVA formulated with either 0.3 or 3 µg of TcdA rRBD. Interestingly, even at a dose as low as 0.3 µg, TcdA rRBD induced at least a 10-fold increase in OVA-specific IgG titers over those obtained with OVA alone ([S6 Fig](#)). The increase in anti-OVA responses was statistically significant ($p < 0.05$). There was no significant difference in the immunogenicity of OVA formulated in TcdA rRBD or alum ([Fig 10A](#)). Interestingly, antisera obtained from mice vaccinated 2 times with 2 µg of OVA
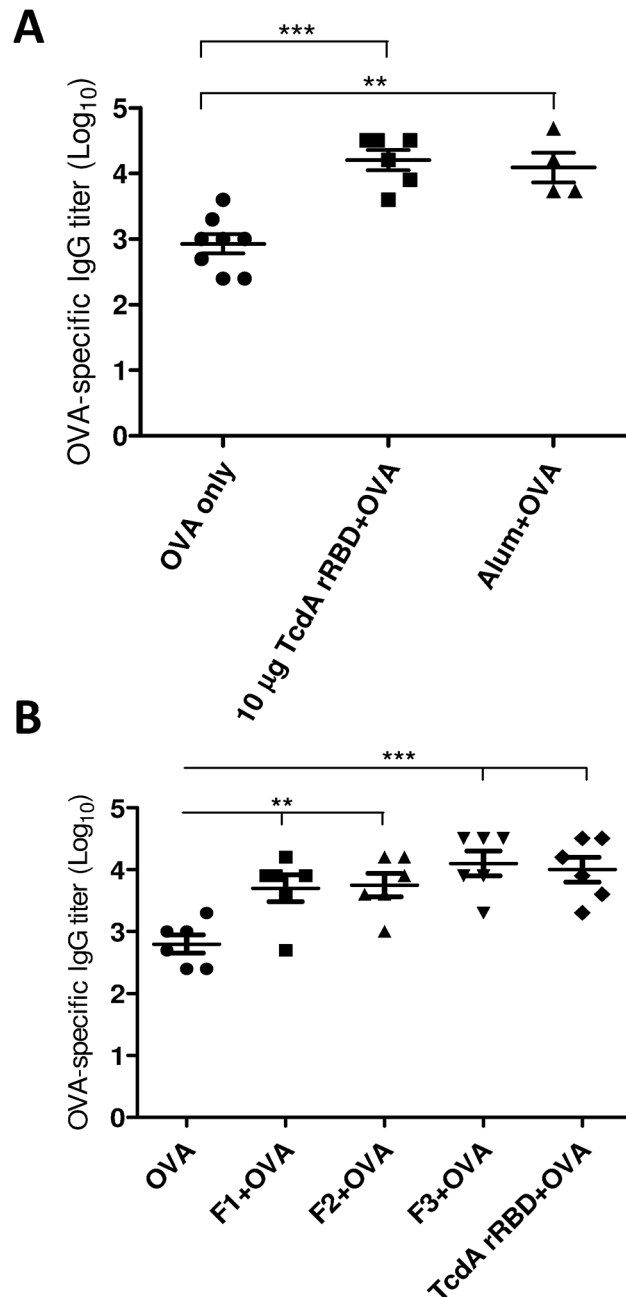
Fig 10. Adjuvant effects of TcdA rRBD and its truncated fragments. To demonstrate the adjuvant effects of TcdA rRBD, enhancement of the anti-OVA IgG response was evaluated by co-administration of TcdA rRBD and OVA. (A) BALB/c mice were immunized with 2 × 2 µg of OVA formulated with or without 10 µg of TcdA rRBD and alum as a positive control. (B) BALB/c mice were immunized with 2 µg of OVA formulated with 10 µg of TcdA rRBD, F1, F2, or F3. The anti-OVA IgG titer was determined by OVA-specific ELISA. The symbols ** and *** indicate $p < 0.01$ and $p < 0.005$, respectively.

doi:10.1371/journal.pone.0135045.g010

formulated with 10 μg of F1, F2, or F3 also demonstrated at least a ten-fold increase in anti-OVA IgG titers over those obtained with OVA alone (*p*<0.01) (Fig 10B). In addition, there was an insignificant difference in adjuvant activity between F1, F2, F3 and TcdA rRBD (Fig 10A). These results indicate that TcdA rRBD and its fragments could be individually used as potent adjuvants for the intramuscular immunization route to enhance immune responses against weak immunogens.

Discussion

To control the increasing incidence of hospital-acquired CDI and curb excessive medical costs, RBD-based CDI vaccines are being developed because recombinant subunit vaccines are cost-effective [11, 24–29, 45]. The clinical isolates of *C. difficile* are rapidly evolving, but sequence analyses of *C. difficile* strains deposited in the NCBI protein database reveal that the amino acid sequences of TcdA RBD share more than 97% identity, and new *C. difficile* strains are primarily BI/NAP1/027-related isolates [46]. To elicit broadly neutralizing antibodies against TcdA, a consensus sequence of TcdA RBD was derived from the NCBI protein database and was found to be identical to the *C. difficile* R20291 strain, a ribotype 027 strain. To study the specific roles and functions of the 7 putative receptor-binding regions, TcdA RBD was divided into three fragments: F1, F2 and F3. Each fragment was purposely designed to contain 3 potential lectin-like receptor-binding (LR) sites. F1 and F2 contain an overlapping LR site #3; F2 and F3 have an overlapping LR site #5 (Fig 1C). It should be noted that the consensus sequence and VPI 10463 reference strain used in all functional assays in this study have 33 synonymous changes within the RBD, including 11, 24 and 16 different amino acids in the F1, F2 and F3 fragments, respectively; these changes are highlighted in Fig 1A. In addition, 12 changes were found within the 7 potential lectin-binding sites, including 1, 5, 3, 2 and 1 amino acids changed in LRs #1, 3, 5, 6 and 7, respectively (Fig 1C). Most changes are found in F2, which may explain why F2 has less potent biochemical and immunological properties (Tables 1 and 2).

The biological and immunological properties of TcdA RBD and its fragments were evaluated using several functional assays [34–36,47–48], and each fragment demonstrated certain interesting properties. The receptor-binding activities obtained from both the Vero/Caco-2 cell-binding assays and FACS analysis (Fig 3A to 3D) provide direct and strong evidence that TcdA rRBD and its fragments (rRBD, F1, F2 and F3) are correctly folded (S1 Fig). These results are consistent with other reports showing that the fragments of RBD containing 5 to 15 short repetitive sequences could form stable folded β-solenoid secondary structures [31]. A novel

Table 2. Summary of biochemical properties of TcdA rRBD and RBD truncated fragments.

Antigen	Biological Properties				
	Cell binding (apparent K_d μM)#		HA activity(pmol)	Cellular uptake	DC maturation(μM)
	Vero cell	Caco-2 cell			
TcdA rRBD	0.14	0.09	0.4	++++	0.2
F1	0.26	0.18	No	+/-	0.8
F2	0.56	0.32	32	++	1
F3	0.16	0.08	2	++++	0.2
TcdA	ND	ND	2	Yes*	Yes*

The apparent K_d is defined as the half-maximal binding of TcdA rRBD to the receptors.

*Yes indicates the information was derived from the literature [40–42, 48].

ND indicates not performed.

doi:10.1371/journal.pone.0135045.t002

finding in the present study is that F1, which contains the first three LR sites, may consist of a unique receptor-binding domain that (a) binds to Vero and Caco-2 cells but is not internalized and (b) does not agglutinate rabbit erythrocytes but still has the ability to activate DC maturation and induce anti-TcdA neutralizing antibody responses. The biochemical properties of F3, which are consistent with other reports [24, 29, 35, 43–45, 47–49], indicate that the last three LR sites contribute to strong HA activity in the rabbit red blood cell agglutination assay, fast and strong binding to both Vero and Caco-2 cells, as shown by FACS analysis, and potent adjuvant activity in enhancing anti-OVA IgG antibody responses. Its rapid internalization properties suggest that F3 could serve as a non-toxic carrier for new drug or vaccine delivery systems with important pharmaceutical applications. F2 possesses lower biological and immunological activities, indicating that the 8 amino acid changes in LR sites #3 (367V→G; 380H→D; 381N→A; 394K→E) and 5 (618D→N; 629H→D; 630N→A; 699Y→S) may be important for the biological and immunological properties of the RBD. Based on the results, these changes (i) affected and reduced the binding between F2 and the monoclonal antibody PCG-4 (Fig 2D), which recognizes an epitope located within the F2 fragment [50]; (ii) might have decreased F2 cell-binding activity (Fig 3D) and HA activity (Table 2); and (iii) certainly influenced the quality of the functional antibodies induced by F2 in the animal immunogenicity study in which F2 elicited no protection against TcdA (VPI10463 strain) challenge (Table 1).

The Vero and Caco-2 cell-binding assays with FACS indicated that TcdA rRBD and its fragments possess different binding activities, and as shown in Fig 2D, the TcdA-specific monoclonal antibody PCG-4 recognized F2 the least. To eliminate the antibody binding affinity problem, FACS analyses were repeated with an anti-His tag antibody, and similar results were obtained (data not shown). This result confirmed that the Vero and Caco-2 cell-binding activities are as follows: F3>F2>F1 (see the insert in Fig 3D).

The HA assay reflects the binding activities of each TcdA rRBD fragment to rabbit erythrocytes. Our current results further demonstrate that the N-terminal (F1) and middle (F2) regions of TcdA rRBD exhibit no or poor HA activity in rabbit erythrocytes. Because F1 has no HA activity and did not internalize after cell binding, F1 will be an excellent choice for the identification of specific cell receptor(s). In addition, we hypothesize that the putative carbohydrate-binding sites LR1/LR2 in F1 and LR6/LR7 in F3 bind to different ligands on the cell surface and may amplify receptor-binding affinity through a multivalent ligand mechanism. Therefore, F1 and F3 should be further truncated to investigate the specific roles and functions of the 7 putative receptor-binding sites of RBD.

TcdA, TcdA RBD and cholera toxin have been shown to possess mucosal adjuvant activity [42–44, 49, 51–53]. The present study has demonstrated that TcdA rRBD and its fragments can individually act as potent adjuvants in the intramuscular immunization route to enhance immune responses against OVA. We also clearly show that 2 µM of either TcdA rRBD or its truncated fragments is sufficient to promote the maturation of BMDCs and increase the secretion of pro-inflammatory cytokines (Figs 6 and 7). CT has been found to essentially promote DC maturation in the presence of its catalytic domain [49–50], but our current results clearly illustrate that TcdA rRBD and its fragments do not require the N-terminal catalytic domain and transmembrane domain of TcdA for DC activation. TcdA rRBD and its fragments have exhibited different levels of adjuvant activity in DC activation and the secretion of pro-inflammatory cytokines. F1 and F2 represent low DC activity, but they alone still possess strong adjuvant activity to elicit anti-RBD antibody responses and enhance immune responses to OVA through a T-cell bystander mechanism. Therefore, the DC activity of the TcdA rRBD fragments may not be the only route to modulate the immune system. Additionally, several reports have shown that TcdA can modulate various immune cells [51–55]. Further studies should be

performed to determine whether TcdA rRBD is also involved in a more complex immune system network.

The present immunogenicity studies show that only toxoid A immunization induces the strongest TcdA neutralization titers and 100% protection (Table 1). The TcdA rRBD and/or rRBD fragments only induce partial protection in the TcdA mouse challenge model. These differences in protection levels can be explained by the following reasons. One is that other regions in TcdA are important and involved in protection against the toxin in the mouse challenge model and may be required for vaccine development. Another reason is that the amino acid sequences of immunogens (TcdA rRBD and its fragments) are derived from the 027 strain and are different from the challenge VPI 10463 strain. Thirty-three amino acid changes within RBD (Fig 1A) may be sufficient to influence the induction of a protective functional cross-neutralizing antibody response. In addition, a low dosage (10 µg) of TcdA rRBD and its fragments was used in the present study compared to other previous reports, in which different dosages, adjuvants, immunization routes and/or vectors were used and could result in different levels of protection in the toxin mouse challenge model [22–29]. The current literature [24,29,36] has indicated that toxin A or toxin A-derived fragments alone cannot induce a protective immune response against live *C. difficile* bacteria in the hamster challenge model. In fact, our preliminary results (Huang et al., unpublished results) indicated that TcdA RBD combined with TcdB RBD can induce efficient protection against *C. difficile* bacteria challenge in hamster models.

Overall, the current study has demonstrated that the biochemical properties of F3, which are consistent with other reports [24, 29, 42–44], indicate that the last three LR sites contribute to strong HA activity in the rabbit red blood cell agglutination assay, rapid and strong binding to both Vero and Caco-2 cells, as shown by FACS analysis, and potent adjuvant activity to enhance anti-OVA IgG antibody responses. F1, F2 and F3 have similar short repetitive amino acid sequences and putative oligosaccharide-binding sites (Fig 1B and 1C) but have dissimilar biochemical and immunological properties. Future studies should investigate which amino acids in these repetitive sequences are responsible for their biochemical functions and TLR agonist activity. As TcdA rRBD, F1 and F3 can elicit immune protective responses against *C. difficile* toxin A, TcdA rRBD and its fragments are certainly potential components for future candidate vaccines against *C. difficile*-associated diseases.

Supporting Information

S1 Fig. The secondary structure of TcdA rRBD and its fragments. (A) CD spectra of TcdA rRBD and its fragments (F1, F2 and F3). (B) The thermal stability curves of TcdA rRBD and its fragments analyzed using CD spectra based on the values at $\theta_{230\ nm}$.
(PDF)

S2 Fig. Vero cell-binding abilities of TcdA rRBD and its truncated fragments. After TcdA rRBD fragments were incubated with Vero cells for 30 min, the TcdA rRBD fragments were characterized by immunoblot analysis using an anti-TcdA specific monoclonal antibody. Two protein concentrations (2 and 6 µM) were used in the cell-binding assay.
(PDF)

S3 Fig. Cellular uptake of TcdA rRBD, F1 and F3 through the clathrin-dependent pathway. Chlorpromazine (CPZ) was used to inhibit TcdA rRBD, F1 and F3 internalization. To confirm that the cellular uptake was receptor-mediated clathrin-dependent endocytosis, CPZ was added into the cell-binding medium, and TcdA rRBD, F1 and F3 internalization was inhibited. The internalization signals for TcdA rRBD and its fragments into Vero cells were evaluated by confocal microscopy at 5, 15, and 30 min. The images were collected from a single stack in the

central region of the *z* axis. Green fluorescence signals represent the locations of TcdA rRBD, F1 and F3. Nuclei were stained with DAPI and are shown in blue.
(PDF)

S4 Fig. Mouse anti-RBD antibody responses elicited by different dosages of TcdA rRBD.
(A) BALB/c mice were immunized three times with 3, 10 or 30 μg of TcdA rRBD, and alum formulation served as the positive control. Anti-RBD titers at 0, 2, 4, 6, and 8 weeks were determined by RBD-specific ELISA. (B) Specific anti-RBD IgG isotypes and IgA were analyzed with the sera obtained from the 6th week post-immunization.
(PDF)

S5 Fig. Immunogenicity study with TcdA rRBD and its truncated fragments with alum.
BALB/c mouse anti-RBD antibody responses elicited by 3 × 10 μg of either TcdA rRBD or its fragments formulated with alum. Anti-RBD IgG titers at 6 weeks were determined by RBD-specific ELISA.
(PDF)

S6 Fig. Adjuvant effects of TcdA rRBD. To demonstrate the adjuvant effects of TcdA-RBD, the increase in the anti-OVA IgG response was evaluated via co-administration of TcdA rRBD and OVA. BALB/c mice were immunized with 2 μg of OVA formulated with either 0.3 or 3 μg of TcdA rRBD or alum as a positive control. The anti-OVA IgG titer was determined by OVA-ELISA.
(PDF)

S1 File. Supporting Information files for Figs 3, 4, 6, 7, 8, 9 & 10 are in the Compressed/ZIP File Archive.
(ZIP)

Acknowledgments

Author Contributions

Conceived and designed the experiments: J-HH C-HL PC-SC. Performed the experiments: J-HH Z-QS S-PL K-NH C-CC. Analyzed the data: J-HH Z-QS C-HL L-KS PC-SC. Contributed reagents/materials/analysis tools: J-HH Z-QS K-NH C-HL L-KS PC-SC. Wrote the paper: J-HH PC-SC.

References

1. Knoop FC, Owens M, Crocker IC (1993) *Clostridium difficile*: clinical disease and diagnosis. Clin Microbiol Rev 6: 251–265. PMID: 8358706

2. Lyerly DM, Krivan HC, Wilkins TD (1988) *Clostridium difficile*: its disease and toxins. Clin Microbiol Rev 1:1–18. PMID: 3144429

3. Kelly CP, LaMont JT (2008) *Clostridium difficile*—more difficult than ever. N Engl J Med 359:1932–1940. doi: 10.1056/NEJMra0707500 PMID: 18971494

4. McDonald LC, Killgore GE, Thompson A, Owens RC, Kazakova SV, Sambol SP, et al. (2005) An epidemic, toxin gene–variant strain of *Clostridium difficile*. N Engl J Med 353: 2433–2441. PMID: 16322603

5. He M, Miyajima F, Roberts P, Ellison L, Pickard DJ, Martin MJ, et al. (2013) Emergence and global spread of epidemic healthcare-associated *Clostridium difficile*. Nat Genet 45:109–113 doi: 10.1038/ng.2478 PMID: 23222960

6. Sun X, Savidge T, Feng H (2010) The enterotoxicity of *Clostridium difficile* toxins. Toxins 2:1848–1880. doi: 10.3390/toxins2071848 PMID: 22069662

7. Kuehne SA, Cartman ST, Heap JT, Kelly ML, Cockayne A, Minton NP (2010) The role of toxin A and toxin B in *Clostridium difficile* infection. Nature 46:7711–713.

8. Davies AH, Roberts AK, Shone CC, Acharya KR (2011) Super toxins from a super bug: structure and function of *Clostridium difficile* toxins. Biochem J 436:517–526. doi: 10.1042/BJ20110106 PMID: 21615333

9. Pruitt RN, Chambers MG, Ng KK, Ohi MD, Lacy DB (2010) Strcutural organization of the functional domains of *C. difficile* toxins A and B. Proc Natl Acad Sci USA 107:13467–72. doi: 10.1073/pnas.1002199107 PMID: 20624955

10. Albesa-Jove D, Bertrand T, Carpenter EP, Swain GV, Lim J, Zhang J, et al. (2010) Four distinct structural domains in *C. difficile* toxin B visualized using SAXA. J Mol Biol 396:1260–70. doi: 10.1016/j.jmb.2010.01.012 PMID: 20070948

11. Humphreys DP, Wilcox MH (2014) Antibodies for treatment of *Clostridium difficile* infection. Clin Vaccine Immunol 21:913–923. doi: 10.1128/CVI.00116-14 PMID: 24789799

12. Wult M, Noren T, Ljungh A, Akerlund T (2012) IgG antibody response to toxins A and B in patients with *Clostridium difficile* infection. Clin Vaccine Immunol 19:1552–1554. doi: 10.1128/CVI.00210-12 PMID: 22787196

13. Aronsson B, Granstrom M, Molby R, Nord CE (1985) Serum antibody response to *Clostridium difficile* toxins in patients with *Clostridium difficile* diarrhoea. Infection 3:97–101.

14. Kyne L, Warny M, Qamar A, Kelly CP (2001) Association between antibody response to toxin A and protection against recurrent *Clostridium difficile* diarrhoea. Lancet 357:189–193. PMID: 11213096

15. Monaghan T, Robins A, Knox A, Sewell HF, Mahida YR (2013) Circulating antibody and memory B-cell responses to *C. difficile* toxins A and B in patients with *C. difficile*-associated diarrhoea, inflammatory bowel disease and cystic fibrosis. PLoS One 8:e74452. doi: 10.1371/journal.pone.0074452 PMID: 24058568

16. Fernie DS, Thomson RO, Batty I, Walker PD (1983) Active and passive immunization to protect against antibiotic associated caecitis in hamsters. Dev Biol Stand 53:325–332. PMID: 6873474

17. Giannasca PJ, Zhang Z-x, Lei W-d, Boden JA, Giel MA, Monath TP, et al. (1999) Serum antitoxin antibodies mediate systemic and mucosal protection from *Clostridium difficile* disease in hamsters. Infect Immun 67:527–538. PMID: 9916055

18. Taylor CP, Tummala S, Molrine D, Davidson L, Farrell RJ, Lembo A, et al. (2008) Open-label, doseescalation phase I study in healthy volunteers to evaluate the safety and pharmacokinetics of a human monoclonal antibody to *Clostridium difficile* toxin A. Vaccine 26:3404–3409. doi: 10.1016/j.vaccine.2008.04.042 PMID: 18502001

19. Lowy IMD, Molrine D, Leav BA, Blair BM, Baxter R, Gerding DN, et al. (2010) Treatment with monoclonal antibodies against *Clostridium difficile* toxin. N Engl J Med 362:197–205. doi: 10.1056/NEJMoa0907635 PMID: 20089970

20. Torres JF, Lyerly DM, Hill JE, Monath TP (1995) Evaluation of formalin-inactivated *Clostridium difficile* vaccines administered by parenteral and mucosal routes of immunization in hamsters. Infect Immun 63:4619–4627. PMID: 7591115

21. Kink JA, Williams JA (1998) Antibodies to recombinant *Clostridium difficile* toxins A and B are an effective treatment and prevent relapse of *C. difficile*-associated disease in a hamster model of infection. Infect Immun 66:2018–2025. PMID: 9573084

22. Sauerborn M, Leukel P, von Eichel-Streiber C (1997) The C-terminal ligand-binding domain of *Clostridium difficile* toxin A (TcdA) abrogates TcdA-specific binding to cells and prevents mouse lethality. FEMS Microbiol Lett 155:45–54. PMID: 9345763

23. Seregin SS, Aldhamen YA, Rastall DP, Godbehere S, Amalfitano A (2012) Adenovirus-based vaccination against *Clostridium difficile* toxin A allows for rapid humoral immunity and complete protection from toxin A lethal challenge in mice. Vaccine 30:1492–1501. doi: 10.1016/j.vaccine.2011.12.064 PMID: 22200503

24. Tian JH, Fuhrmann SR, Kluepfel-Stahl S, Carman RJ, Ellingsworth L, Flyer DC (2012). A novel fusion protein containing the receptor binding domains of *C. difficile* toxin A and toxin B elicits protective immunity against lethal toxin and spore challenge in preclinical efficacy models. Vaccine 30:4249–4258. doi: 10.1016/j.vaccine.2012.04.045 PMID: 22537987

25. Ryan ET, Butterton JR, Smith RN, Carroll PA, Crean TI, Calderwood SB (1997) Protective immunity against *Clostridium difficile* toxin A induced by oral immunization with a live, attenuated Vibrio cholerae vector strain. Infect Immun 65:2941–2949. PMID: 9199470

26. Ward SJ, Douce G, Figueiredo D, Dougan G, Wren BW (1999) Immunogenicity of a *Salmonella typhimurium* aroA aroD vaccine expressing a nontoxic domain of *Clostridium difficile* toxin A. Infect Immun 67:2145–2152. PMID: 10225867

27. Gardiner DF, Rosenberg T, Zaharatos J, Franco D, Ho DD (2009) A DNA vaccine targeting the receptor-binding domain of *Clostridium difficile* toxin A. Vaccine 27:3598–3604. doi: 10.1016/j.vaccine.2009.03.058 PMID: 19464540

28. Permpoonpattana P, Hong HA, Phetcharaburanin J, Huang JM, Cook J, Fairweather NF, et al. (2011) Immunization with *Bacillus* spores expressing toxin A peptide repeats protects against infection with *Clostridium difficile* strains producing toxins A and B. Infect Immun 79:2295–2302. doi: 10.1128/IAI.00130-11 PMID: 21482682

29. Leuzzi R, Spencer J, Buckley A, Brettoni C, Martinelli M, Tulli L, et al. (2013) Protective efficacy induced by recombinant *Clostridium difficile* toxin fragments. Infect Immun 81:2851–2860. doi: 10.1128/IAI.01341-12 PMID: 23716610

30. Dove CH, Wang SZ, Price SB, Phelps CJ, Lyerly DM, Wilkins TD, et al. (1990) Molecular characterization of the *Clostridium difficile* toxin A gene. Infect Immun 58:480–488. PMID: 2105276

31. Ho JG, Greco A, Rupnik M, Ng KK (2005) Crystal structure of receptor-binding C-terminal repeats from *Clostridium difficile* toxin A. Proc Natl Acad Sci USA 102:18373–18378. PMID: 16344467

32. Greco A, Ho JG, Lin SJ, Palcic MM, Rupnik M, Ng KK (2006) Carbohydrate recognition by Clostridium difficile toxin A. Nat Struct Mol Biol 13:460–461. PMID: 16622409

33. Pruitt RN, Lacy DB (2012) Toward a structural understanding of Clostridium difficile toxins A and B. Front Cell Infect Microbiol 2:28. doi: 10.3389/fcimb.2012.00028 PMID: 22919620

34. Krivan HC, Clark GF, Smith DF, Wilkins TD (1986) Cell surface binding site for *Clostridium difficile* enterotoxin: evidence for a glycoconjugate containing the sequence Gal alpha 1-3Gal beta 1-4GlcNAc. Infect Immun 53:573–581. PMID: 3744552

35. Dingle T, Wee S, Mulvey GL, Greco A, Kitova EN, Sun J, et al. (2008). Functional properties of the carboxy-terminal host cell-binding domains of the two toxins, TcdA and TcdB, expressed by *Clostridium difficile*. Glycobiology 18:698–706. doi: 10.1093/glycob/cwn048 PMID: 18509107

36. Huang JH, Wu CW, Lien SP, Hsiao KN, Leng CH, Lin YH, et al. (2015) Biochemical and immunological characterizations of the receptor binding domain of C. difficile toxin B. J Vaccines Vaccin 6:276–284.

37. Wren BW, Russell RR, Tabaqchali S (1991) Antigenic cross-reactivity and functional inhibition by antibodies to *Clostridium difficile* toxin A, *Streptococcus mutans* glucan-binding protein, and a synthetic peptide. Infect Immun 59:3151–3155. PMID: 1715320

38. Lutz MB, Kukutsch N, Ogilvie AL, Rossner S, Koch F, Romani N, et al. (1999) An advanced culture method for generating large quantities of highly pure dendritic cells from mouse bone marrow. J Immunol Methods 223:77–92. PMID: 10037236

39. Burger S, Tatge H, Hofmann F, Genth H, Just I, Gerhard R (2003) Expression of recombinant *Clostridium difficile* toxin A using the Bacillus megaterium system. Biochem Bioph Res Co 307:584–588.

40. Papatheodorou P, Zamboglou C, Genisyuerek S, Guttenberg G, Aktories K (2010) Clostridial glucosylating toxins enter cells via clathrin-mediated endocytosis. PLOS ONE 5:e10673. doi: 10.1371/journal.pone.0010673 PMID: 20498856

41. Olling A, Goy S, Hoffmann F, Tatge H, Just I, Gerhard R (2011) The repetitive oligopeptide sequences modulate cytopathic Potency but are not crucial for cellular uptake of *Clostridium difficile* toxin A. PLoS ONE 6:e17623. doi: 10.1371/journal.pone.0017623 PMID: 21445253

42. Lee JY, Kim H, Cha MY, Park HG, Kim YJ, Kim IY, et al. (2009) *Clostridium difficile* toxin A promotes dendritic cell maturation and chemokine CXCL2 expression through p38, IKK, and the NF-kappaB signaling pathway. J Mol Med (Berl) 87:169–180.

43. Castagliuolo I, Sardina M, Brun P, DeRos C, Mastroto C, Lovato L, et al. (2004) *Clostridium difficile* toxin A carboxyl-terminus peptide lacking ADP-ribosyltransferase activity acts as a mucosal adjuvant. Infect Immun 72:2827–2836. PMID: 15102793

44. Brun P, Scarpa M, Grillo A, Palu G, Mengoli C, Zecconi A, et al. (2008) *Clostridium difficile* TxAC314 and SLP-36kDa enhance the immune response toward a co-administered antigen. J Med Microbiol 57:725–31 doi: 10.1099/jmm.0.47736-0 PMID: 18480329

45. Hussack G, Arbabi-Ghahroudi M, van Faassen H, Songer JG, Ng KK, MacKenzie R, et al. (2011) Neutralization of *Clostridium difficile* toxin A with single-domain antibodies targeting the cell receptor binding domain. J Biol Chem 286:8961–8976. doi: 10.1074/jbc.M110.198754 PMID: 21216961

46. Stabler RA, Dawson LF, Valiente E, Cairns MD, Martin MJ, Donahue EH, et al. (2012) Macro and micro diversity of *Clostridium difficile* isolates from diverse sources and geographical locations. PLOS ONE 7:e31559. doi: 10.1371/journal.pone.0031559 PMID: 22396735

47. Ward SJ, Douce G, Dougan G, Wren BW (1999) Local and systemic neutralizing antibody responses induced by intranasal immunization with the nontoxic binding domain of toxin A from *Clostridium difficile*. Infect Immun 67:5124–5132. PMID: 10496886

48. Gerhard R, Frenzel E, Goy S, Olling A (2013) Cellular uptake of *Clostridium difficile* TcdA and truncated TcdA lacking the receptor binding domain. J Med Microbiol 62:1414–1422. doi: 10.1099/jmm.0.057828-0 PMID: 23558138

49. Yeh CY, Lin CN, Chang CF, Lin CH, Lien HT, Chen JY, et al. (2008) C-terminal repeats of *Clostridium difficile* toxin A induce production of chemokine and adhesion molecules in endothelial cells and promote migration of leukocytes. Infect Immun 76:1170–1178. PMID: 18160482

50. Frey SM, Wilkins TD (1992) Localization of two epitopes recognized by monoclonal antibody PCG-4 on Clostridium difficile toxin A. Infect Immun 60:2488–2493. PMID: 1375199

51. Gagliardi MC, Sallusto F, Marinaro M, Langenkamp A, Lanzavecchia A, De Magistris MT (2000). *Cholera* toxin induces maturation of human dendritic cells and licences them for Th2 priming. Eur J Immunol 30:2394–2403. PMID: 10940931

52. Lavelle EC, Grant G, Pusztai A, Pfuller U, O'Hagan DT (2001) The identification of plant lectins with mucosal adjuvant activity. Immunology 102:77–86. PMID: 11168640

53. Shen A (2012) Clostridium difficile toxins: mediators of inflammation. J Innate Immun 4: 149–158. doi: 10.1159/000332946 PMID: 22237401

54. Kim JM, Lee JY, Yoon YM, Oh YK, Youn J, Kim YJ (2006) NF-kappa B activation pathway is essential for the chemokine expression in intestinal epithelial cells stimulated with Clostridium difficile toxin A. Scand J Immunol 63: 453–460. PMID: 16764699

55. Flegel WA, Muller F, Daubener W, Fischer HG, Hadding U, Northoff H (1991) Cytokine response by human monocytes to Clostridium difficile toxin A and toxin B. Infect Immun 59: 3659–3666. PMID: 1910012